EFFECT OF NIGHT SKY BACKGROUNDS ON OPTICAL MEASUREMENTS

GEOPHYSICS CORPORATION OF AMERICA
700 COMMONWEALTH AVENUE, BOSTON 15, MASSACHUSETTS

EFFECT OF NIGHT SKY BACKGROUNDS ON OPTICAL MEASUREMENTS

FINAL REPORT
to
Itek Corporation
P.O. No. 8110
for
Lincoln Laboratory
P.O. No. A-2231
AF19(604)-4559

Prepared by: R. M. Chapman
Robert M. Chapman
Robert O'B. Carpenter
Robert O'B. Carpenter

Approved by: Richard Coons
Richard Coons
Vice-President,
Marketing

6 March 1959

Geophysics Corporation
of
America

EFFECT OF NIGHT SKY BACKGROUNDS ON OPTICAL MEASUREMENTS

Prepared By

R. O'B. Carpenter and R. M. Chapman

Geophysics Corporation of America

TABLE OF CONTENTS

Page

I. GENERAL PROPERTIES OF BACKGROUNDS 1

A. Introductory Statement of the Problem 1
B. Properties of the Night Source 1
C. Sources of Night Sky Backgrounds 5
D. Star Counts, Star Catalogues, and Stellar Color. 6
E. Table of Number of Stars at Each Magnitude 11
F. Absolute Magnitude of the Diffuse Component 17
G. Twilight and Moonlight 17
H. Attenuation by the Earth's Atmosphere 24
I. The Seeing of Point Sources Through the Atmosphere 28
J. Man-Made Lighting. 31

II. STUDY OF THE SLIT SPECTROGRAPH WITH MULTIPLE DETECTORS. 33

A. Properties of the Tracking System. 33
B. Cell Noise Limitations-1P21 Photomultiplier. 35
C. Required Size of Spectral Dispersing Element 37
D. Statistical Fluctuations in the Steady Night Background. . . 41
E. Estimate of Trajectory Speed, Time of Star Passage, and Power Spectrum 45
F. Evaluation of the Venetian Blind Clutter-Rejection Chopper . 48
G. Summary of Performance of the Slit Spectrograph. 51

III. SLITLESS OBJECTIVE SPECTROGRAPH 53

A. The Cassegrain Telescope-Objective Spectrograph 53
B. Tracking the Objective Spectrograph. 55
C. Four Telescope Array 56
D. Stationary Objective Spectrograph 56

IV. INFRARED DETECTION 59

LIST OF ILLUSTRATIONS

Figure		Page
1.	Gaslight Prediction	3
2.	Reference Target Spectrum	4
3.	Stellar Color Nomograph	9
4.	Relative Contribution to Average Starlight	14
5a.	Average Diffuse Radiation from Zenith, 0.3 to 1.3 Microns	18
5b.	Average Diffuse Radiation from Zenith, 1.3 to 5.0 Microns	19
6.	High Resolution Night Sky Spectra	20
7.	Zenith Twilight Intensity	21
8.	Zenith Moonlight Intensity	22
9.	Correction Factor for Moon Phase	23
10.	Atmospheric Transmission, 0.3 to 1.3 Microns	25
11.	Atmospheric Transmission, 1.2 to 5.0 Microns	26
12.	Factors Determining Size of Dispersion Element	39
13.	Noise Equivalent Signal	44
14.	Star Pulse Shapes and Frequency Spectra	47

LIST OF TABLES

Table		Page
1.	The Temperature of the Stars	10
2.	Stellar Distribution of Magnitudes (Whole Sky)	13
3.	Contributions to the Average Total Size of the Star Images at Night	31

ABSTRACT

A review is given of the sources and magnitudes of the night sky backgrounds, from 0.3 to 5 microns particularly as they might interfere with the observation of the spectrum of a small missile re-entering the atmosphere. Distributions of stellar magnitude and color, zodiacal and galactic scattered light, air glow, twilight, moonlight, and man-made lighting are discussed.

Application is made of the background magnitude data to estimate the limitation of the threshold of large telescope-spectrometers using 1P21, PbS, and other detectors. Objective and slit-type spectrographs are considered, including the requirements for, and effect of, tracking precision.

Accepted for the Air Force
Franklin C. Hudson
Chief, Lincoln Laboratory Office

SECTION I

GENERAL PROPERTIES OF BACKGROUNDS

A. Introductory Statement of the Problem

In Project Meteor, a five-inch re-entry object will be injected into the atmosphere nearly vertically downward at a velocity of about 25,000 feet per second. The purpose of this study will be to review the design considerations for a telescope, spectrometer, and means for recording the spectrum in absolute intensity units of the "gaslight" emitted by this re-entering object.

Restrictions set by the observing test range (at Wallops Island) will probably limit the range of the observing equipment to about 100 miles for a land site, or 40 miles for a shipboard site. In either case the weakness of the source signal will lead to a requirement for rather large telescopes and spectrometers. Careful design of the equipment parameters will be required to obtain a maximum amount of information at a reasonable size and cost of equipment.

In this analysis, major emphasis will be placed on the interfering effect of the night sky background. However, it will first be necessary to review the calculation of the expected received radiation levels, required telescope and spectrometer fields, and apertures, etc. in order to provide the data on which a quantitative evaluation of background interference can be based.

B. Properties of the Target Source

In Figures 1 and 2, an estimate has been made of the expected absolute intensity and spectrum of the emission from this re-entry body. These estimates were made from published theoretical calculations and shock tube experiments on the volume emissivity of heated air as a function of temperature and density by the Avco Research Laboratory. To predict the emission from any re-entering object, an aerodynamic prediction of the flow field (that is,

the profile of temperature and density about the object), is first required as a function of velocity and ambient pressure. Then the emissivity data may be applied to estimate the total emission into any aspect direction by a calculation of the volume integral of emissivity over the flow field.

The results of this approximate calculation are shown in Figure 1. It is seen that the total "gaslight" emission is low at the top and bottom of the trajectory. Interaction between speed, deceleration, and ambient pressure lead to a maximum in the "gaslight" at about a 150,000 foot altitude for this particular object shape and trajectory. This peak is estimated to be about 9 watts/steradian. The aspect has not been stated, nor the shape of the spectrum, nor the variation in either spectral shape or absolute magnitude with aspect. Assuming that the emission is isotropic, the above figure leads to a total emission of about 110 watts at peak.

In the present experiments it will be highly desirable to be able to trace the course of the emission growth and decay in both total intensity and spectral distribution. Thus the spectral equipment must have far more capability than just enough to detect the above peak values. For example, from the data of Figure 1, it appears that with 0.1 watts/steradian capability one might obtain most of the re-entry spectrum from at least 100,000 to 250,000 feet, perhaps a little higher. In succeeding calculations this will be used as the reference value for estimates of required telescope and spectrometer sizes.

In order to estimate the energy available to any particular narrow spectral band in the equipment, it is further necessary to know the spectral distribution of the emission. From at least one estimate, for a quite different shape and speed, the spectral distribution of Figure 2 was predicted. This spectral shape was also verified to some extent by measurements in shock tubes.

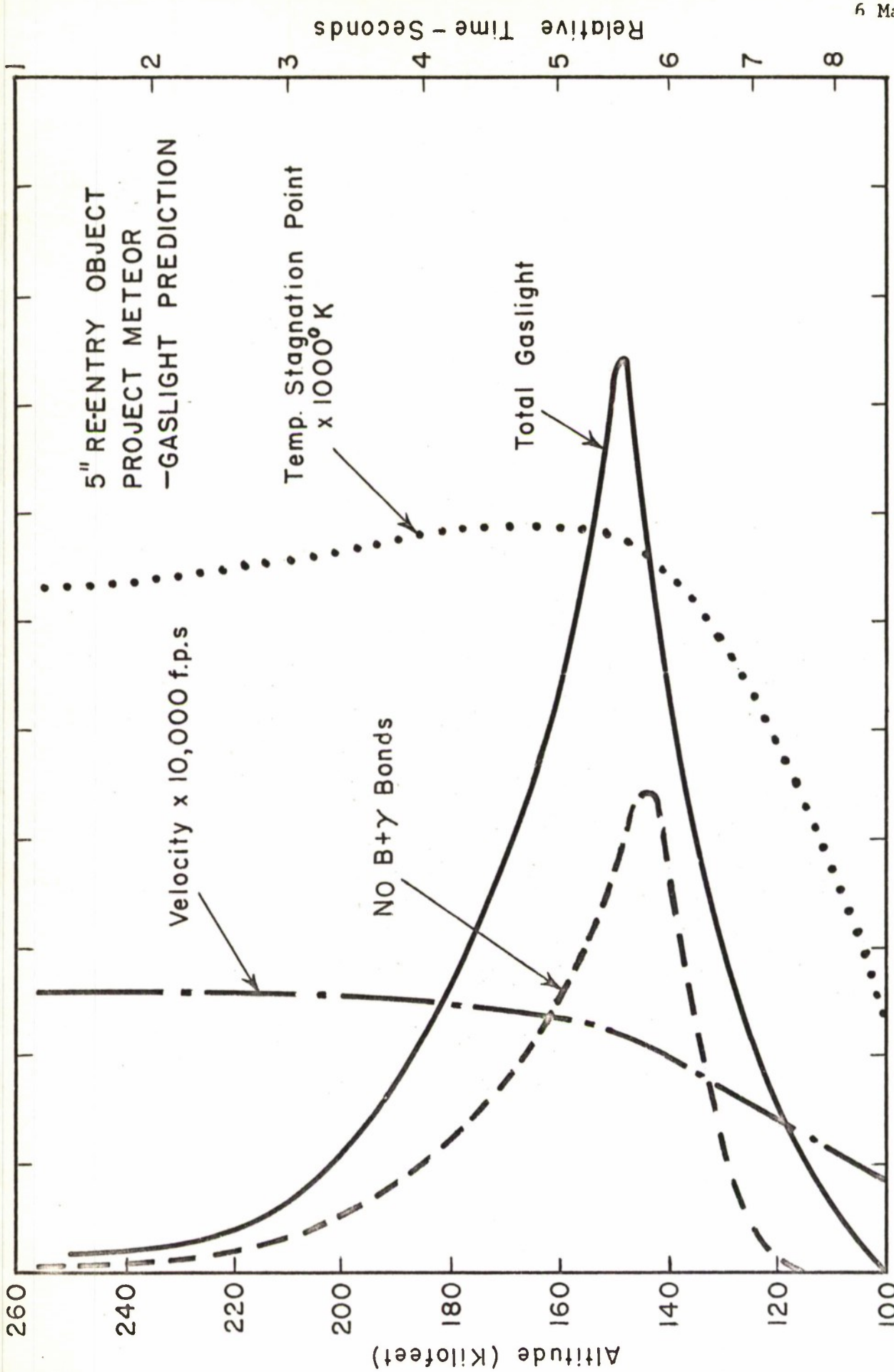

Figure 1. Gaslight Prediction

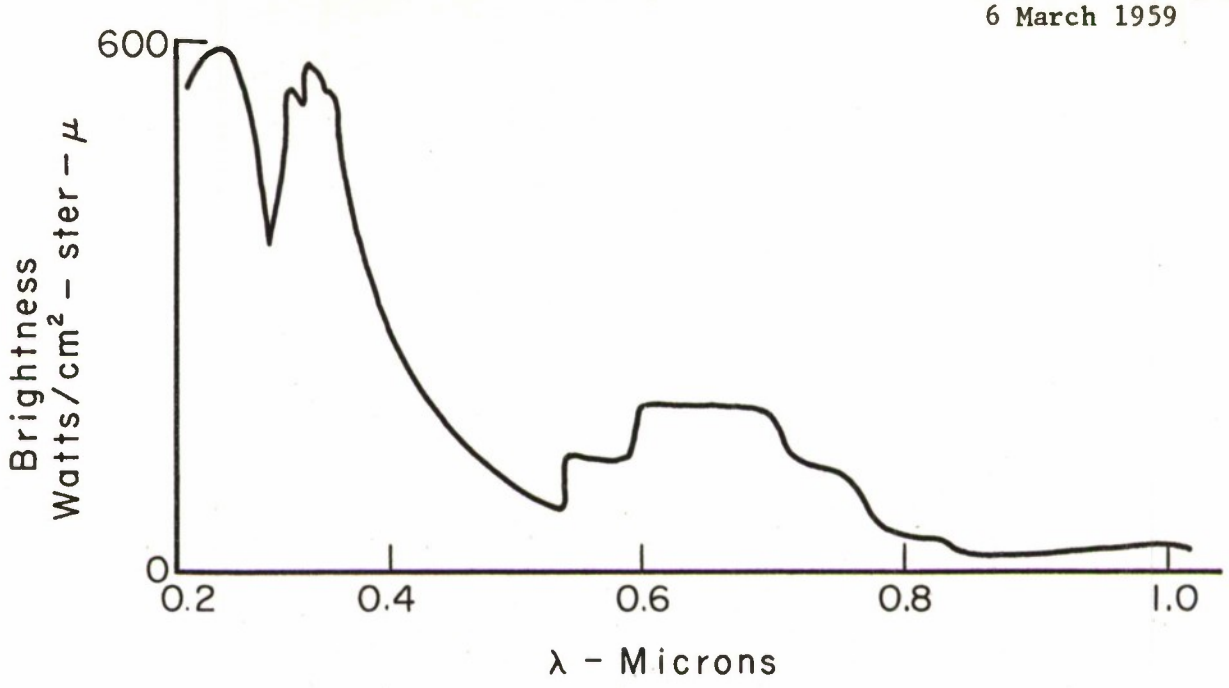

Emission From 1 cm^3 Air at 8000°K, p/p_o = 0.85
(Avco)

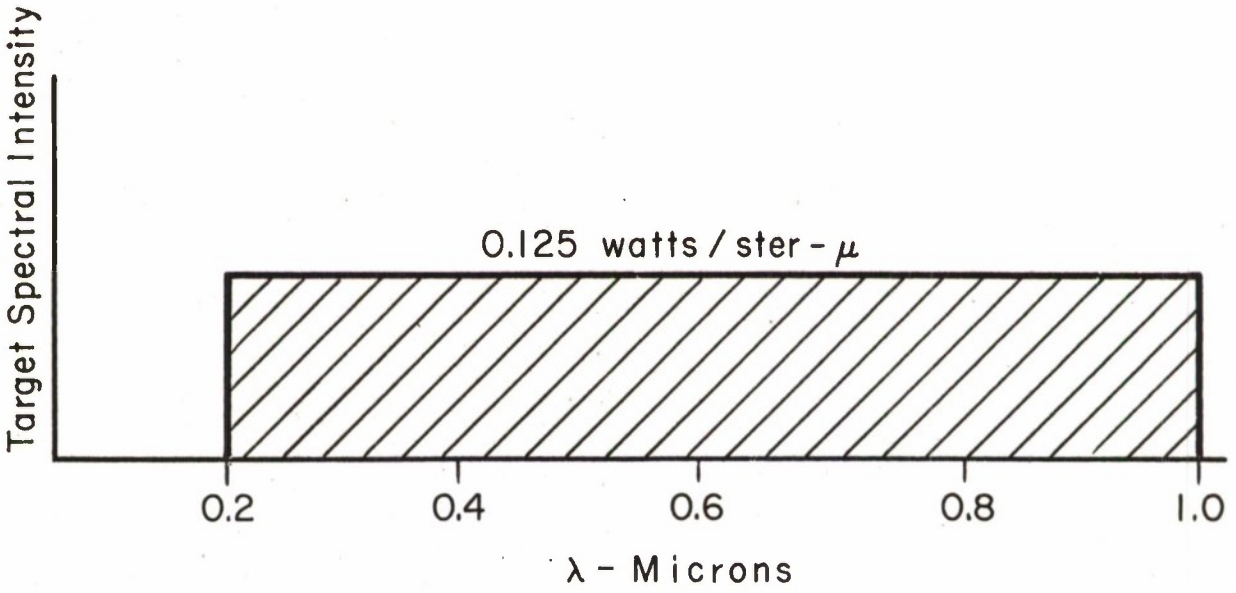

Assumed Reference Target Spectrum (when target is at 100,000 and 250,000 Feet)

Figure 2. Reference Target Spectrum

It is not certain, however, that this spectral distribution is applicable to the present experiments. Lacking any further information on the spectrum, it will be assumed for simplicity that the total estimate is uniformly distributed in a spectral band from 0.2 to 1.0 microns. This leads to a spectral emission of 0.125 watts/steradian-micron as a reference value.

Taking 100 miles (1.61×10^7 centimeters) as the reference range, the spectral flux density at the aperture of the telescope is (neglecting any atmospheric attenuation):

$$(SFD) = \frac{0.125}{(1.61 \times 10^7)^2} = 4.8 \times 10^{-16} \text{ (watts/sq cm-micron)} \qquad (1)$$

Since a zero magnitude star at 0.55 micron emits a spectral flux density of 3.0×10^{-12} watts/cm^2-u for all spectral classes, the target at 0.55u would be rated a magnitude of +4.6 at peak intensity, or + 9.5 at the above reference value.

C. Sources of Night Sky Backgrounds

S.K. Mitra, in The Upper Atmosphere, second edition, 1952, estimates the contributions from the various sources of night sky emissions as follows:

Star light, direct and scattered	30 per cent
Zodiacal light	15 per cent
Galactic light	5 per cent
Luminescence of the night sky (air glow)	40 per cent
Scattered light from the last three sources	10 per cent

These estimates are for the luminous or visible portions of the energy, and are for conditions several hours after twilight, with no moon. (Twilight and moonlight will be later considered separately.) Man-made illuminations are also excluded.

The zodiacal light is mainly due to sunlight scattered by the rarified upper layers of the earth's atmosphere, and thus appears primarily in a prism

about 60° high by 35° wide rising from the horizon at the ecliptic. The galactic light is starlight emitted or scattered by interstellar dust in the Milky Way, and thus is largely concentrated in the galaxy. The "air glow" is emitted by atmospheric molecules about 50 to 200 km in altitude. If the direction of view during an experiment avoids both the ecliptic and the galactic, a good bit of the zodiacal and galactic light can be avoided, and the major diffuse night emission will come from the "air glow."

Since all these components of night emission vary in different ways with direction and time of view, atmospheric, and meteorological conditions, the best that can be done in this short study is to abstract from the literature certain mean or average values as an order of magnitude guide in designing the re-entry telescope-spectrometers for roughly estimating the threshold and contrast set by the background illumination.

For the purposes of the current application, it will be useful to divide the night sky background into the "star component" and the "diffuse component," which will be treated in the following sections of this report.

D. Star Counts, Star Catalogues, and Stellar Color

Many major observatories have extensive programs in cataloguing the stars, their position on celestial coordinates, visual and/or photographic magnitude, spectral color or class, and other determined characteristics. One of the best, easily available, publications is the Atlas Coeli Skalnate Pleso (Skalnate Pleso Atlas of the Heavens) published in 1951 by A. Becvar of the Czechoslovakian Observatory at Skalnate Pleso (distributed in the United States by the Sky Publishing Corp., 60 Garden Street, Cambridge, Mass.). This catalogue and star chart is widely used for general field identification and data reducing work by astronomers, and is recommended for use on this project. A copy has been delivered to Lincoln Laboratory under this contract.

This catalogue lists all the celestial objects to just beyond the 6th magnitude (more than 10,000 objects), with their celestial coordinates as of 1950, annual variation, proper motion, visual magnitude, spectral class, parallax, and radial velocity. The associated star chart is a plotted map

of the entire heavens in 16 plates which show every object brighter than magnitude 7.75 (thus more than the catalogue), with a code in one-half magnitude steps based on the diameter of the plotted circle.

The Atlas Enclipticalis 1950, a more complete catalogue in 32 larger scale charts just published by the same author (A. Becvar) has also been ordered (available only by direct order to Prague). This covers only declinations + 30 to - 30, but includes all objects to the 9th magnitude with some additional 9 to 10. The main use of the chart and catalogue will be as follows: an actual or predicted target trajectory can be reduced to celestial coordinates (as of 1950) and plotted on the appropriate star chart. The magnitude and location of any suspected star pulse interferences are then readily observed on the chart. Recourse to the catalogue will be necessary only if one wishes to identify the interfering visual magnitude to closer than the one-half magnitude steps, or, more important, if one wishes to estimate the interfering magnitude at some wavelength removed from the visible, for which one will require knowledge of the spectral color or class.

The stellar magnitude m is a logarithmic scale for indicating the relative radiant flux density received at the surface of the earth from a star and is defined in the following way

$$m = -2.5 \log_{10} \frac{u}{u_o}$$

or

$$\frac{u}{u_o} = 10^{-0.4m}$$

The log constant, 2.5, makes exactly 5 magnitudes equal an intensity ratio of 100, and is approximately consistent with ancient historical magnitude scales. Relative magnitudes can be defined for radiation of any wavelength, or for a broad spectral receiver. However, relative magnitudes will be a function of the spectral shape of the star's emission and the receiver's sensitivity.

The most extensive accurate determinations and most star catalogues are based on the visual magnitude, that is, in visual photometric units, such

as lumens/sq cm. The luminous flux density q_o received from a star of zero magnitude is

$$q_o = 2.1 \times 10^{-10} \text{ lumens/sq cm}$$

The spectra of most stars which have been observed, as of the sun, will approximate a black body at some representative temperature, as modified by the stellar and earth atmospheres. For a rough approximation to the stellar spectrum, lacking individual information, about the best one can do is estimate the stellar temperature and assume a black body spectrum. Astronomers have adopted the Draper classification for stellar spectra, in which the designations from higher to lower temperature run: O, B, A, F, G, K, M, R, N, S. For finer divisions, a single decimal digit following the class can divide each class into ten parts, while in some classes a distinction in spectrum or temperature has been found between "giant," g, and "dwarf," d, stars. Thus the complete designation gG2 means a giant star of spectrum shape roughly 0.2 of the way between class G0 and K0.

Measurements of effective stellar temperatures are reviewed in the text, Astronomy, Volume II, by Russell, Dugan, and Stewart, Table XXX, p. 753, which is reproduced here, in Table 1, in order of decreasing temperature. For simplicity, in the last two columns we have suggested a reduction of the 20 full classes to a series of only eight temperatures. The re-entry spectroscopic measurements will be concerned with very narrow spectral bands, essentially monochromatic, so our requirement is for a procedure of determining "monochromatic magnitude" from the "visual magnitude." This has been done by means of the nomograph of Figure 3. This is a plot of

$$\frac{N \quad (\lambda, T)}{B\ (T)}$$

for each of the eight reference stellar temperatures, where

N (λ, T) is spectral radiance of a black body at absolute temperature, T (the Planck function) in watts/sq cm - steradian-micron).

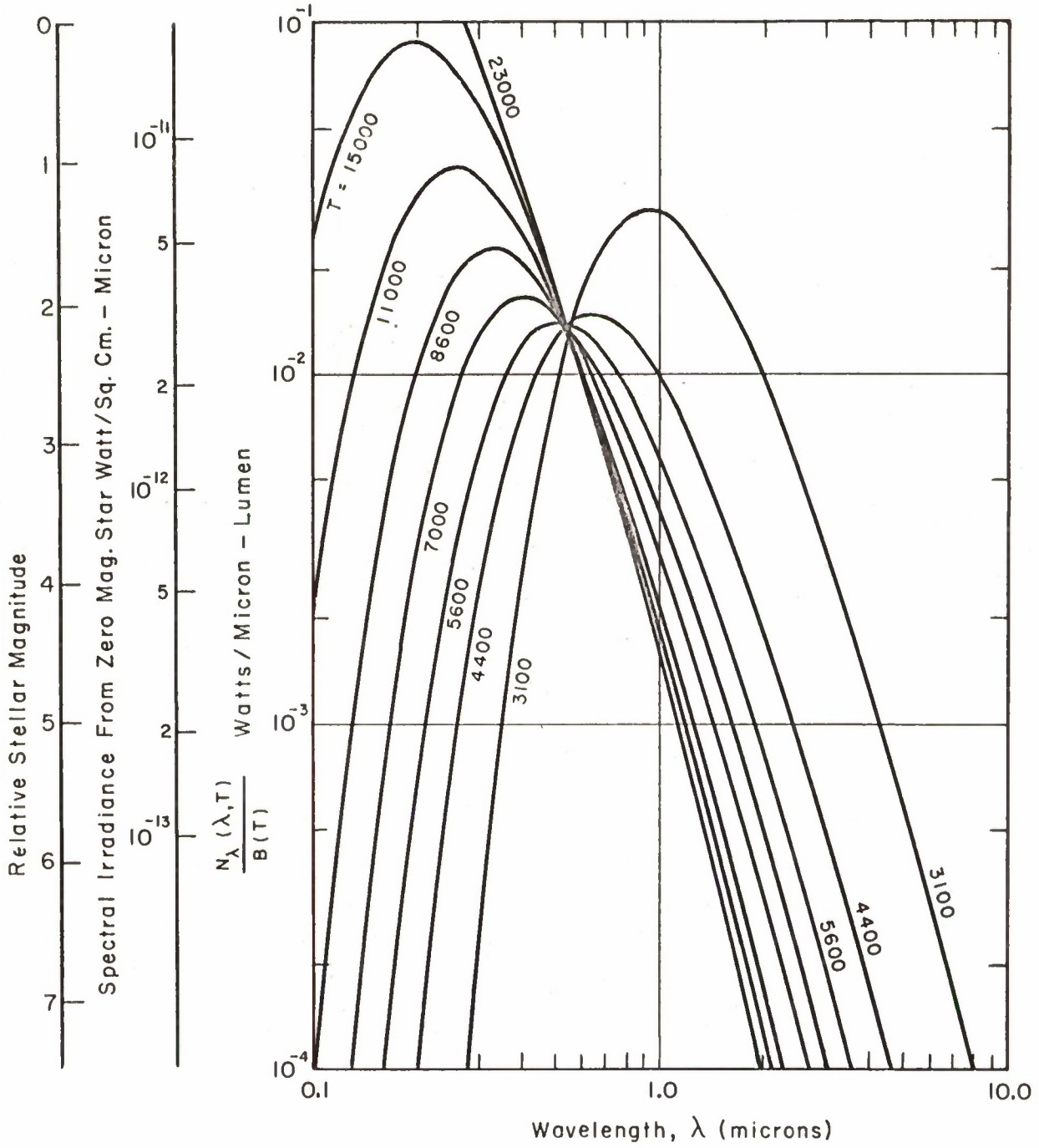

Figure 3. Stellar Color Nomograph

TABLE 1

THE TEMPERATURE OF THE STARS

(from Russell, Dugan, Stewart, Vol. II, Table XXX, p. 753)

Draper Classification	Color Index	Heat Index	Engergy Curves	Diameters	Adopted Temperature	Limited Scale for Use with Fig. 10		
						Class	% Stars	Reference Temperature
0					?> 25000		*	
B0	23000				23000	B0		23000
B5	15000				15000	B5	2	15000
A0	11200		12500	10000	11000	A0		11000
A5	8600			8000	8000	A5	29	8600
F0	7400				7400			
F5	6500		8000		6500	F	9	7000
dG0	6000				6000			
dG0, dG5	5500	5500	5800		5600	G'	21	5600
dK0	5100				5100			
gG5	4700				4700			
dK5	4400				4400	K'	33	4400
gK0	4100	4200		4300	4200			
gK5, dM	3300		3000	3800	3400			
gM2	3050	3100	2700	3100	3100	M'	6	3100
gM5		2750	2500	2650	2700			
N	2200	2700			2600		*	

*Less than 1% in these classes.

B (T) is the luminance, or photometric brightness, of the same black body in lumens/sq cm - steradian.*

This ratio has the units watts/micron-lumen, and gives the absolute spectral distribution of flux (watts/micron) for the quantity of radiation which gives a visible sensation of 1 lumen. A second ordinate scale has been multiplied by $q_o = 2.1 \times 10^{-10}$ lumens/sq cm. Thus the middle scale for each class gives the absolute spectral irradiance (watts/sq cm - micron) produced just outside the earth's atmosphere by a zero magnitude star.

This nomograph shows very clearly how two stars which are the same magnitude at one wavelength or spectral band may have a quite different relative magnitude at some other wavelength, or as observed by some other detector.

The unofficially adopted standard of 2.1×10^{-10} lumens/sq cm obviously applies only to the visual magnitude. For the purposes of establishing a reference zero magnitude for other wavelengths, it has been agreed that a star of spectral class dGO, or an effective color temperature of 11,000°K, shall have the same magnitude for all colors, wavelengths or detectors. Thus the curve for 11,000°K on Figure 3 is the reference irradiance for zero magnitude at any wavelength. The star catalogues give the visual magnitude and the spectral class (or effective temperature). The "monochromatic magnitude" is then obtained by subtracting the "color index" which is the reference magnitude at the star's temperature relative to the 11,000°K curve on Figure 3. The additional ordinate "m-scale" helps in quickly determining this "color index" for eight temperatures shown.

E. Table of Number of Stars at Each Magnitude

A table of the distribution in magnitude of all the stars in the heavens is helpful in giving a general or average intuition about several parameters of interest in evaluating the interfering pulses from the stellar background: (a) the average relative occurrence of interfering pulses of any given size, (b) the relative contribution of each magnitude of the average night sky

*These quantities can be obtained, for example, from Progress Report Number AF-51, Harvard Computation Laboratory, "Tables of Blackbody Radiation Fucntions," M. Pivovonsky, June 1958; or from Smithsonian Physical Tables 9th Ed., W. E. Forsythe, or from other tables of black body functions.

light, and (c) the relative contribution of each magnitude to the rms noise amplitude. This will be done first for visual magnitudes since this is the information most readily available.

Such a count, taken from Russell, Dugan, and Stewart, is shown in Table 2. The second column shows the given information and the number of stars brighter than a given magnitude. The third column, by subtraction, gives the number of stars m from m-1 to m. The fourth column gives the relative intensity, A_m (or amplitude) of each group.

The relative contribution of each magnitude to the total starlight is proportional to $n_m A_m$. This is shown in column five and plotted versus magnitude in Figure 4. It is seen that the contribution peaks at about the 12th magnitude.

The sum of column five is 274 equivalent stars of - 0.5 magnitude in the listing to the 20th magnitude. Correcting to zero magnitude reference and adding a few weaker than 20th by extrapolation of Figure 4, it appears that the total starlight in the visual is equivalent to approximately:

450 stars of zero magnitude in the whole sky.
35.8 stars of zero magnitude per steradian.
0.0109 stars of zero magnitude per square degree.

If N is the total number of stars in the sky, randomly distributed, and allowance is made for the obliquity factor ($\cos\theta$), the effective luminance produced at the ground is equivalent to N/4 stars at zenith, or

113 stars of zero magnitude, all at zenith.
113 $q_o = 2.38 \times 10^{-8}$ lumens/sq cm (starlight).
or 3.34×10^{-10} watts/sq cm - micron spectral irradiance at 0.55 micron.

These figures run about one-fourth to one-sixth the actual visible light observed from the night sky at a dark location on a clear night. The other contributions come from various diffuse (nonpoint) sources discussed in other sections of this report.

TABLE 2

STELLAR DISTRIBUTION OF MAGNITUDES (WHOLE SKY)

(1) Visual Magnitude m	(2) No. Stars Brighter Than m	(3) No. Stars m - 1 to m n_m	(4) Amplitude Rel. to Zero Magnitude $A_m = 10^{-0.4m}$	(5) Rel. Contr. to Av. Light $n_m A_m$	(6) Rel. Contr. to RMS Fluct. $n_m A_m^2$	(7) $\sum_{-\infty}^{m} n_m A_m^2$	(8) Average Time Betw. Stars Seconds
-1	1	1	2.51	2.51	6.3	6.3	31,400
0	2	1	1	1.00	1.00	7.3	31,400
1	12	10	0.398	3.98	1.58	8.88	3,140
2	37	25	.158	3.95	.624	9.504	1,260
3	135	98	.063	6.17	.39	9.894	321
4	530	395	.0251	9.92	.249	10.143	80
5	1620	1,090	.0100	10.90	.109	10.252	28.8
6	4850	3,230	3.98×10^{-3}	12.85	.051	10.303	9.7
7	1.43×10^{4}	9,450	1.58×10^{-3}	14.9	.0235	10.3265	3.3
8	4.1×10^{4}	26,800	6.3×10^{-4}	16.85	.0106	10.3371	1.17
9	1.17×10^{5}	76,000	2.51×10^{-4}	19.05	.0048	10.3419	0.41
10	3.24×10^{5}	207,000	10^{-4}	20.7	.0021	10.3440	.15
11	8.7×10^{5}	546,000	3.98×10^{-5}	21.75	.00086	10.34486	.057
12	2.27×10^{6}	1.4×10^{6}	1.58×10^{-5}	22.15	.00035	10.34521	.022
13	5.7×10^{6}	3.43×10^{6}	6.3×10^{-6}	21.6	.000136	10.34535	.0092
14	1.38×10^{7}	8.1×10^{6}	2.51×10^{-6}	20.3	.000051	10.34540	.0039
15	3.2×10^{7}	1.82×10^{7}	10^{-6}	18.2	.0000182	10.34542	.0017
16	7.1×10^{7}	3.9×10^{7}	3.98×10^{-7}	15.5	6.2×10^{-6}		.00080
17	1.5×10^{8}	7.9×10^{7}	1.58×10^{-7}	12.5	2.0×10^{-6}	10.34543	.00040
18	2.96×10^{8}	1.46×10^{8}	6.3×10^{-8}	9.2	5.8×10^{-7}		.00022
19	5.6×10^{8}	2.64×10^{8}	2.51×10^{-8}	6.63	1.7×10^{-7}		.000056
20	10^{9}	4.4×10^{8}	10^{-8}	4.40	4.4×10^{-8}		.00003
TOTAL		1.0×10		274.01	10.34543	10.34543	

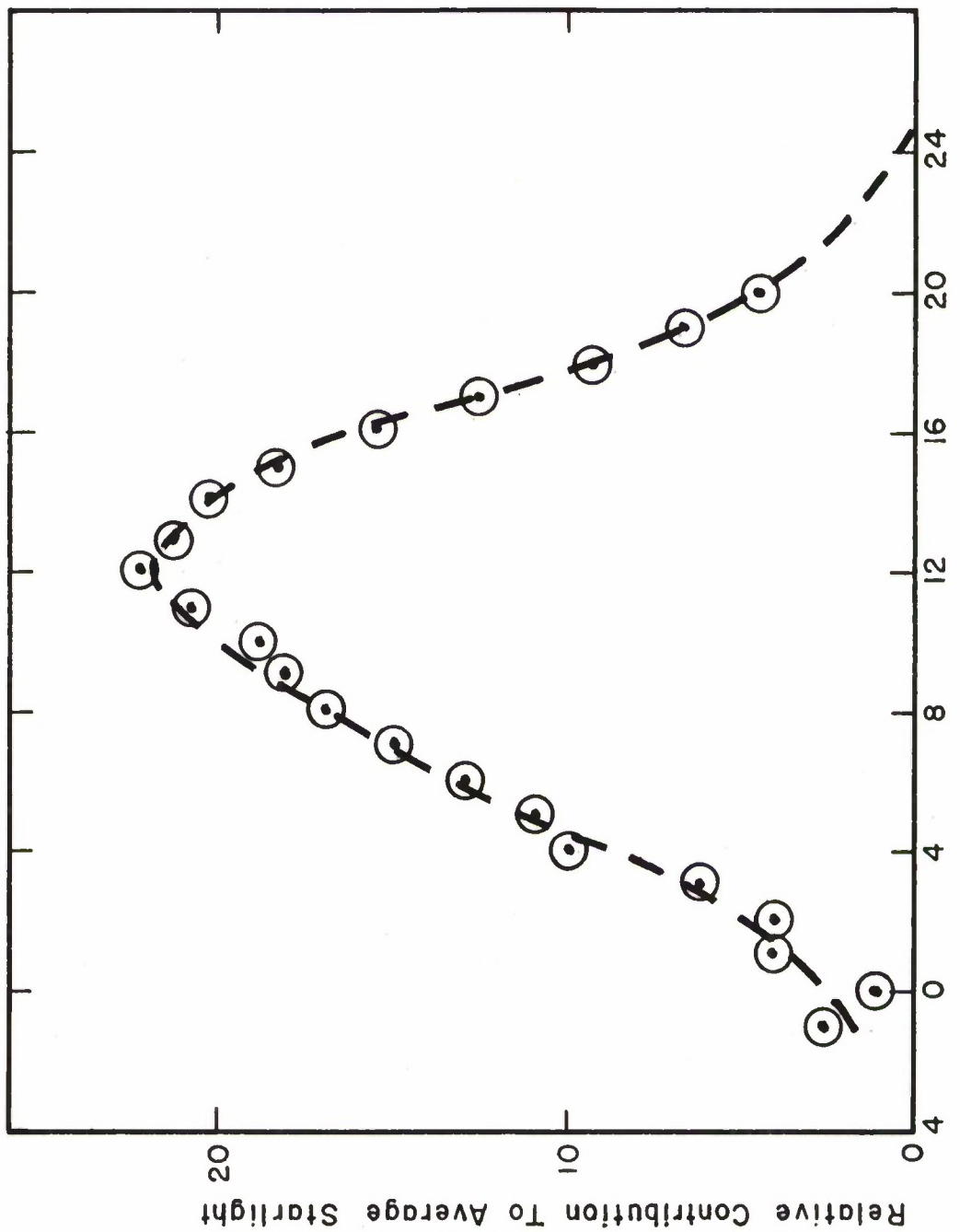

Figure 4. Relative Contribution to Average Starlight

If a field edge of width α radians sweeps the sky uniformly at θ radians per second, the average rate at which the stars enter the field of view is $N_m = \frac{n_m \alpha \theta}{4\pi}$ $\frac{\text{stars}}{\text{second}}$ (Example: $N_m = \frac{10^{-4}}{\pi} n_m$)

The reciprocal of N_m is the average time between star encounters of a given magnitude. A sample computation for $\alpha = 0.01$ radians, $\theta = 0.04$ radians/second is shown in column eight of Table 2. Even for a field of this size, it is seen that an occurrence of a star of the brighter magnitudes is rare, relative to observation times of the order of one-sixth second.

In Section (II, E) the noise power spectrum will be discussed. Some idea of average noise power may be had by considering the data in the distribution table. If δt is the time for a star to cross the field of view, $A_m^2 \delta t$ is the energy in a single pulse. The total noise power is $\Sigma_m N_m A_m^2 \delta t$. Column seven of Table 2 indicates the relative contribution $N_m A_m^2$ for each magnitude and the relative sum for all magnitudes.

For a sufficiently ergodic noise, the "rms" noise amplitude is given by the square root of the noise power. We shall see that these star pulses do not satisfy the ergodic requirement, but let us pursue this agrument with the same numerical example used so far ($T = 1/4$ second). We obtain

$$A_{rms} = \sqrt{\sum_m N_m A_m^2 \; T} = \sqrt{\frac{10^{-4}}{\pi} \times 10.35 \times 1/4}$$

$= 0.009$ stars of magnitude - 0.5.

$= 0.0057$ stars of magnitude zero.

$= 1.68 \times 10^{-14}$ watts/cm^2- micron at 0.55 micron.

This is to be compared with the predicted spectral flux density from the target of 4.8×10^{-16} watts/cm^2-micron.

The signal-to-noise is only 1:35. The noise and the S/N dependent on the spacial structure of the background (e.g., stars) does not depend at all on the telescope aperture, A_o, nor the spectral bandwidth, $\Delta\lambda$. but the S/N does improve inversely with the field angle α . A reduction of the diameter of field of view to about 1/3 milliradian would be sufficient,

on this argument, to reduce the star noise fluctuations to approximately the level of the thermionic cell noise and the fluctuations in the current due to diffuse background. This is without any other form of clutter rejection at all.

The above result has included all the noise power in the square star pulses. But if the overall photometer response time T is greater than the duration of single pulse, $\delta t = \frac{\alpha}{\theta}$, there is a further filtering effect due to the long integration time of the equipment. This has the effect of reducing the noise power by $\delta t/T$, or the amplitude by $\sqrt{\delta t/T}$. In our numerical example with δt = 1/4 second, T = 1/6 second, this effect is small; but if the field of view were significantly reduced, it could become significant. Thus in the region of $\delta t << T$ the average noise power varies as α^{-3}, the "rms amplitude" as $\alpha^{-3/2}$.

Too strict an interpretation should not be applied to the "rms amplitude" calculated from the statistical distribution of star amplitudes in the sky. The average power in the star pulses is correctly calculated, but column 7 of Table 2 shows that the brightest stars contribute the vast majority of the noise power. In fact over 50 per cent comes from Sirius, the single brightest star in the sky. The "noise" from the star pulses is not "white," but rather is dominated by a very few widely separated large pulses.

The concept of "rms amplitude" would have more meaning if we restricted ourselves to those magnitudes for which there is appreciable probability of overlap of star pulses. This magnitude depends on the field of view and the scan speed, but for the sample conditions, is at about the 10th magnitude. Then one could visualize the noise as a "white" substratum overlaid with rare and separated larger pulses.

Viewed in this way, the white noise component from stars weaker than 10th magnitude is less than the noise from other causes in the system which have been discussed. All this is just another way of saying that the principal noise interference problem created by the stars is the few large star pulses at rare intervals coming from the brightest stars in the heavens.

F. Absolute Magnitude of the Diffuse Component

Our estimates for the spectrum of the zenith night emission are abstracted from F. E. Roach, NBS Report No. 5006, "Manual for Photometric Observations of the Airglow during the IGY." Extensive measurements were made to average over times, seasons, and direction of view in the celestial sphere. The result is shown in Figures 5A and B. Since a good portion of the continuum can be avoided by waiting for favorable directions, it appears that except for the narrow, intense Na and OI atomic lines, relatively moderate night sky emissions appear between 0.3 and 1.0 microns. Beginning at 1.0 micron, however, the intense OH molecular bands appear in the "air glow!" Above 2 microns the thermal emission from the dense lower atmosphere obscures the "air glow."

For the purpose of estimating the noise due to the statistical fluctuations in the background quanta, a reference value has been selected for the spectral brightness of the background:

$B_N = 4.4 \times 10^{-10}$ watts/sq cm - steradian-micron at 5500 angstroms.

Figure 6 shows a few miscellaneous high-resolution night sky spectra.

G. Twilight and Moonlight

Data on the additional contributions from twilight and moonlight were obtained from Final Report, Geo-Science, Inc. "Twilight and Airglow Study," Contract AF 19(122)-433, January 1953.

Their results for twilight are reproduced in Figure 7. It appears that at sunset the zenith intensity approaches 10^5 times the night limit, but rapidly falls to the night value of about 200 millimicrolamberts at about one hour after sunset when there is a clear sky.

The full moonlight scattered from the zenith is shown in Figure 8. This varies from 1 to 10 microlamberts as the moon rises from the horizon to 75 degrees. If the moon is less than full, the reduction factors of Figure 9 are to be used.

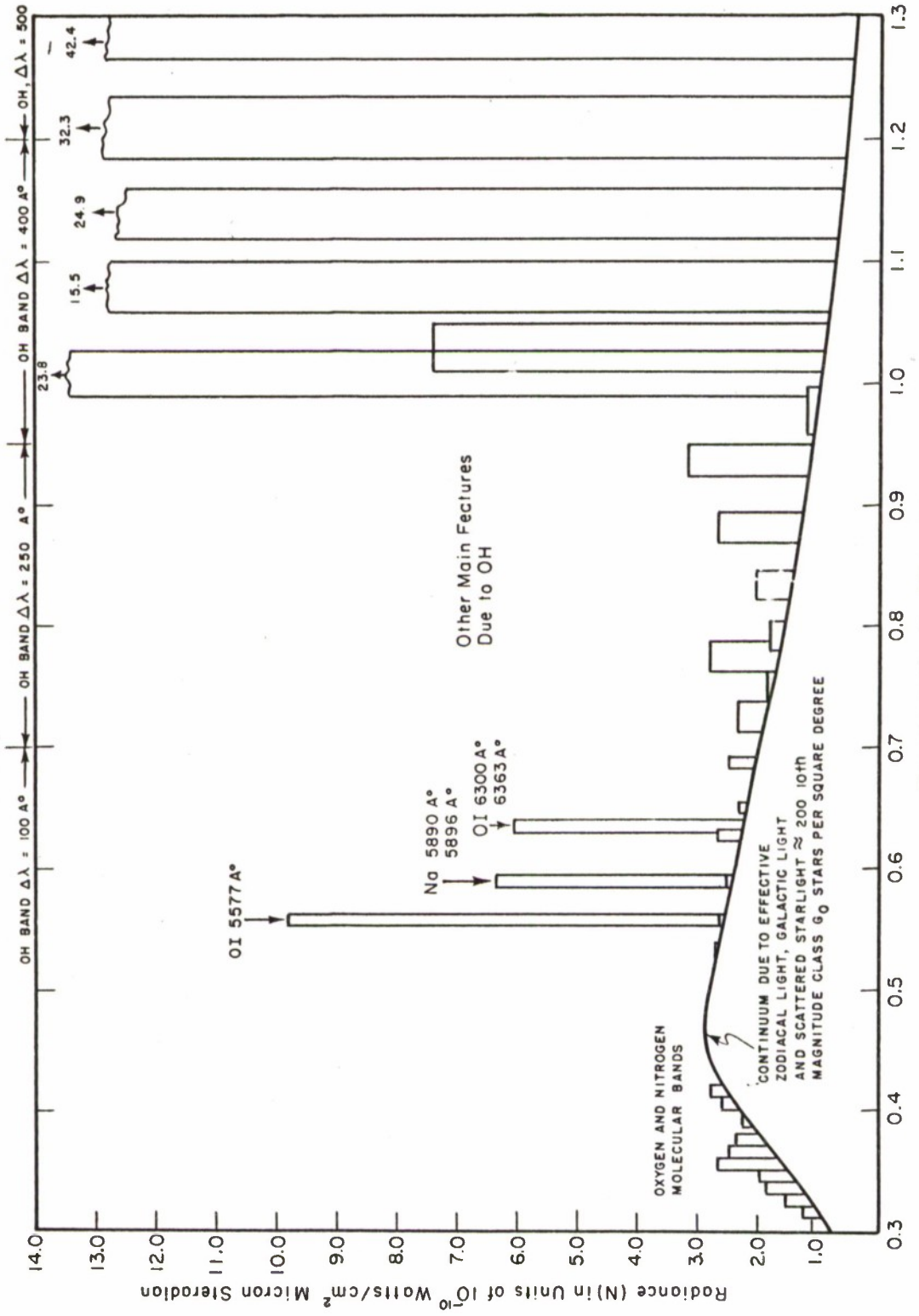

Figure 5a. Average Diffuse Radiation from Zenith, 0.3 to 1.3 Microns

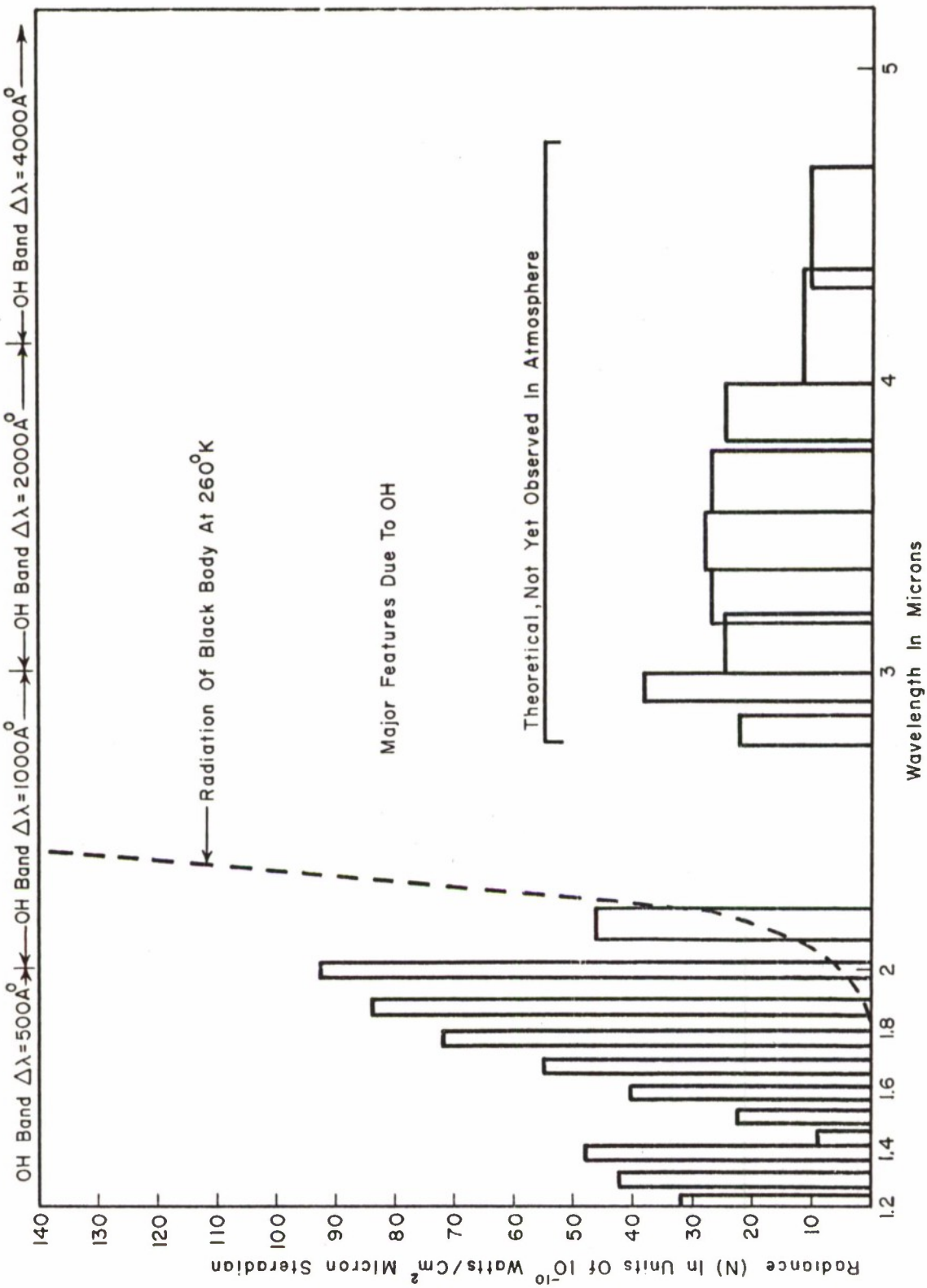

Figure 5b. Average Diffuse Radiation from Zenith, 1.3 to 5.0 Microns

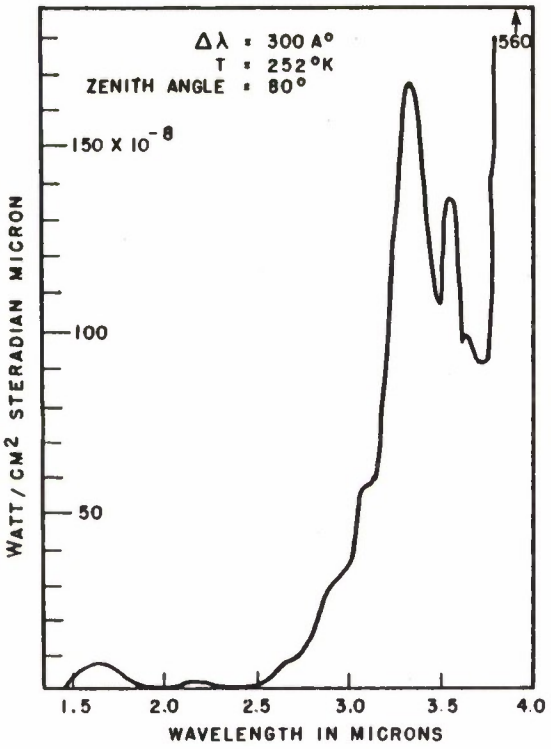

FROM "THE INFRARED SPECTRUM OF THE NIGHT AIRGLOW" NOXON HARRISON AND JONES
J. ATM & TERR. PHYSICS 1959

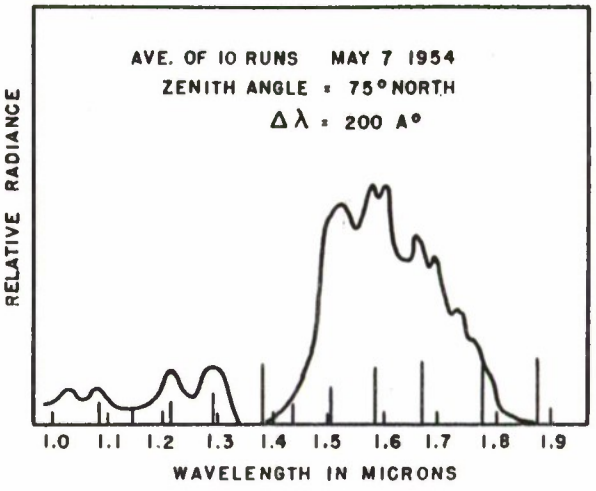

FROM "INFRARED SPECTRUM OF THE NIGHT SKY FROM 1.0 μ TO 2.0μ". GUSH AND JONES
J. ATM. & TERR. PHYSICS 1959

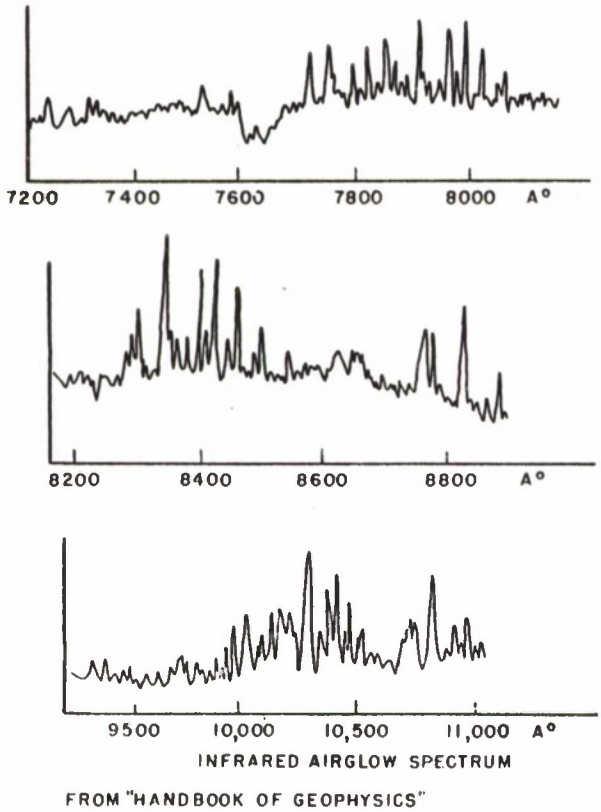

FROM "HANDBOOK OF GEOPHYSICS"

Figure 6. High Resolution Night Sky Spectra

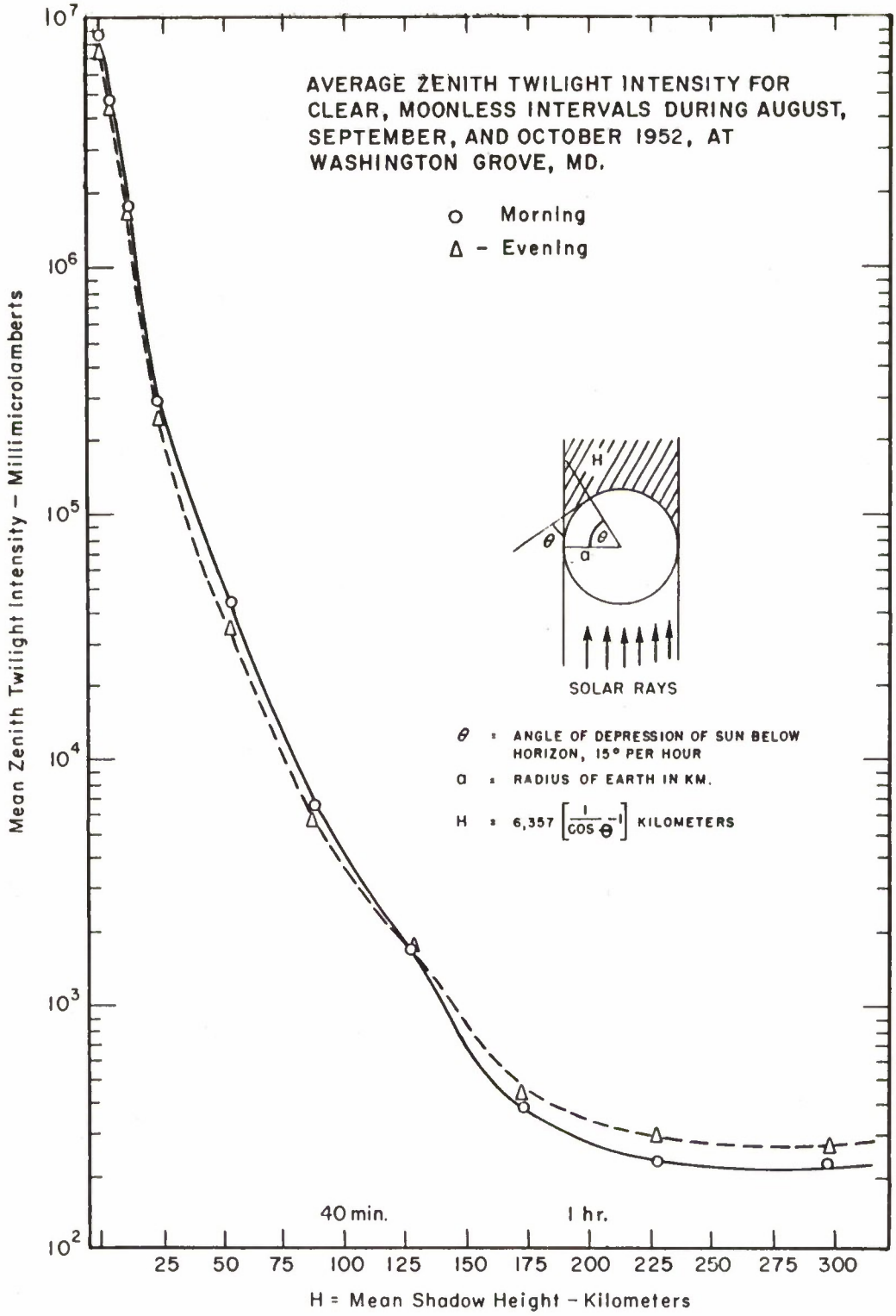

Figure 7. Zenith Twilight Intensity

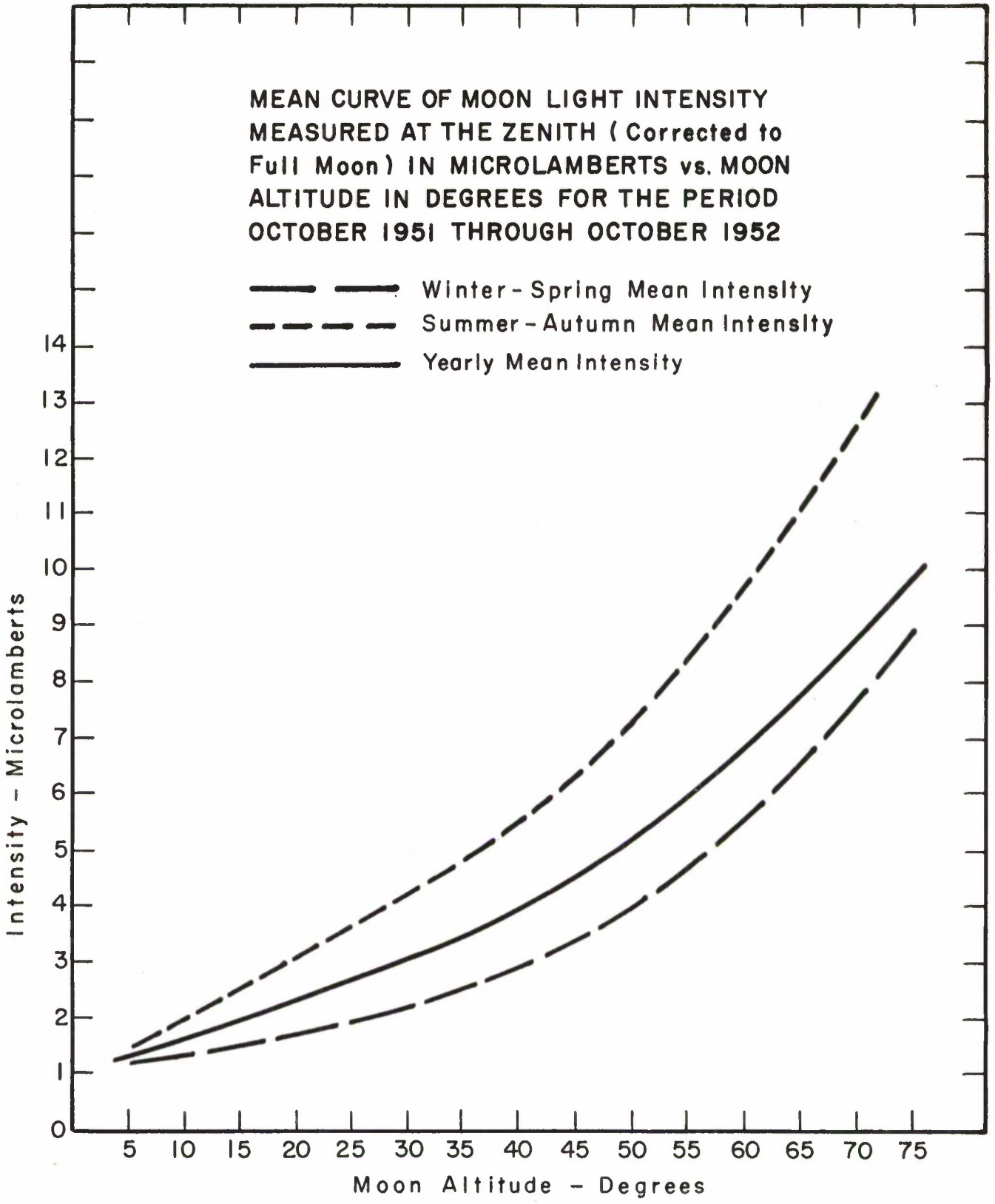

Figure 8. Zenith Moonlight Intensity

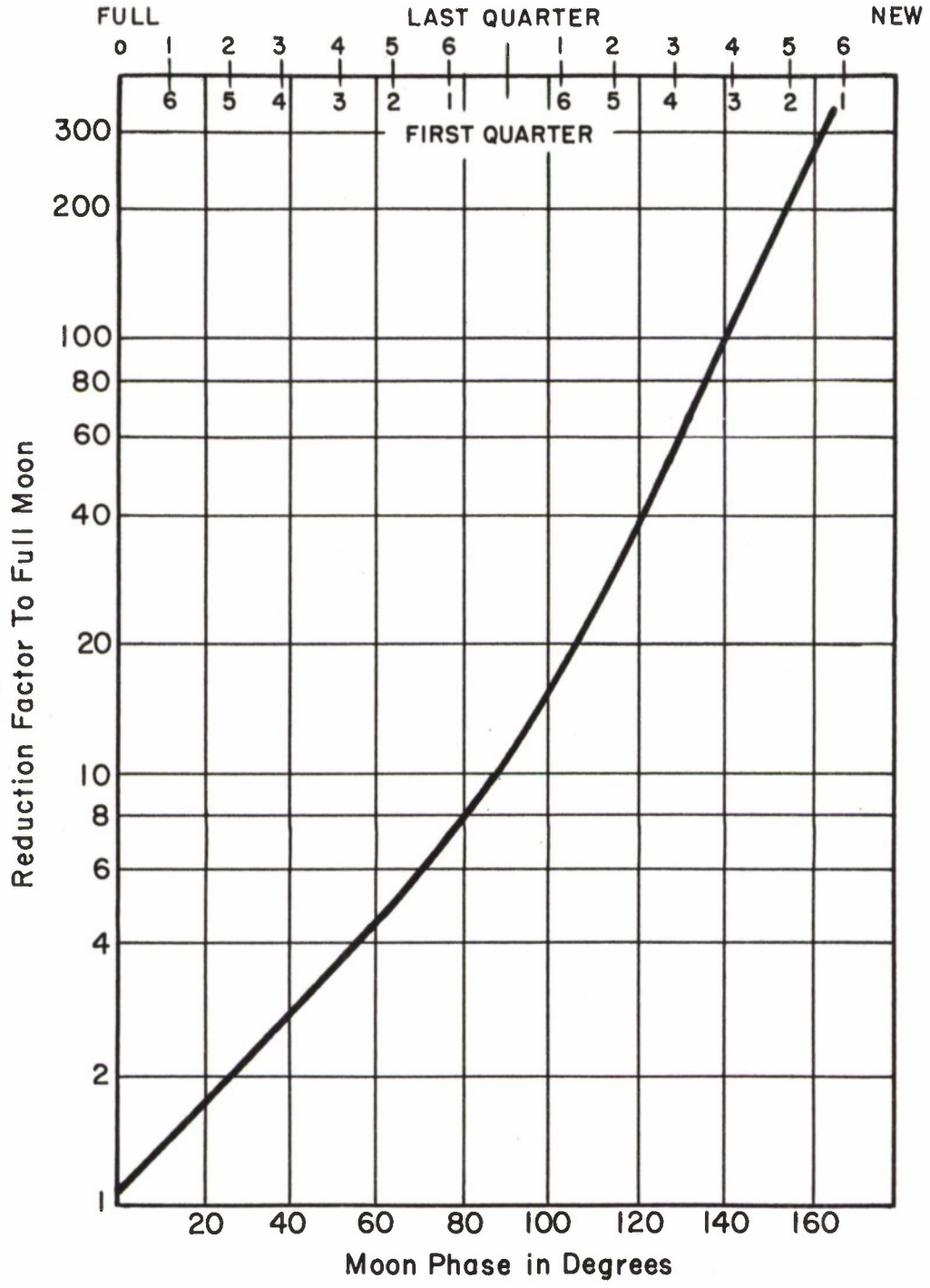

CORRECTION FACTOR TO FULL MOON AGAINST MOON PHASE IN DEGREES

Figure 9. Correction Factor for Moon Phase

The conclusions from these results are that the first hour or two adjoining sunrise or sunset are to be avoided, and that the illumination from a full moon is excessive. Combinations of telescope-moon angle and moon phase can be used, however, which lead to an estimated sky brightness less than 0.2 microlambert. For example, a 120-degree moon phase 40 degrees off the telescope axis appears to be tolerable.

H. Attenuation by the Earth's Atmosphere

The target of observation may in general be considered to be located above a scale height of 5 miles of atmosphere and therefore must be viewed through at least one air mass, even for a zenith angle of 0°. In addition, since the target will be located above most of the earth's ozone layer even at 100,000 feet, the powerful absorption in the ultraviolet from 2000 to 3000 A , in conjunction with atmospheric scattering will prevent any sea level optical observations.[1]

Figures 10 and 11 present a low resolution picture of the transmission of the atmosphere from 0.3 to 5 microns for good visibility conditions at sea level, i.e., greater than 50 miles, and for 2 precipitable centimeters of water vapor in a vertical column above the observation station, i.e., if all the water vapor in a vertical column through the atmosphere were condensed, the thickness of the resulting pool of liquid at N.T.P. would be two centimeters deep. These figures are believed to be roughly representative of attainable conditions at sea level near large bodies of water for spring through fall seasons. Low temperatures tend to reduce the amount of water vapor and give some improvement of transmission in the infrared "window" regions for a given air mass or zenith angle. The data were taken mainly from Moon[2] and others[3] based on years of effort relative to solar constant work. The transport of radiation through the earth's atmosphere

---

1. "Absorption Coefficient of Ozone in the Ultraviolet and Visible Regions," E.C.Y. Inn and Y. Tanaka, J. Opt. Soc. Am., 43 : 870, 1953.

2. "Proposed Standard Solar Radiation Curves for Engineering Use," P. Moon, J. Franklin Institute, 230 : 583, (1940).

3. "Handbook of Geophysics" Geophysics Research Directorate, AFCRC, 1957.

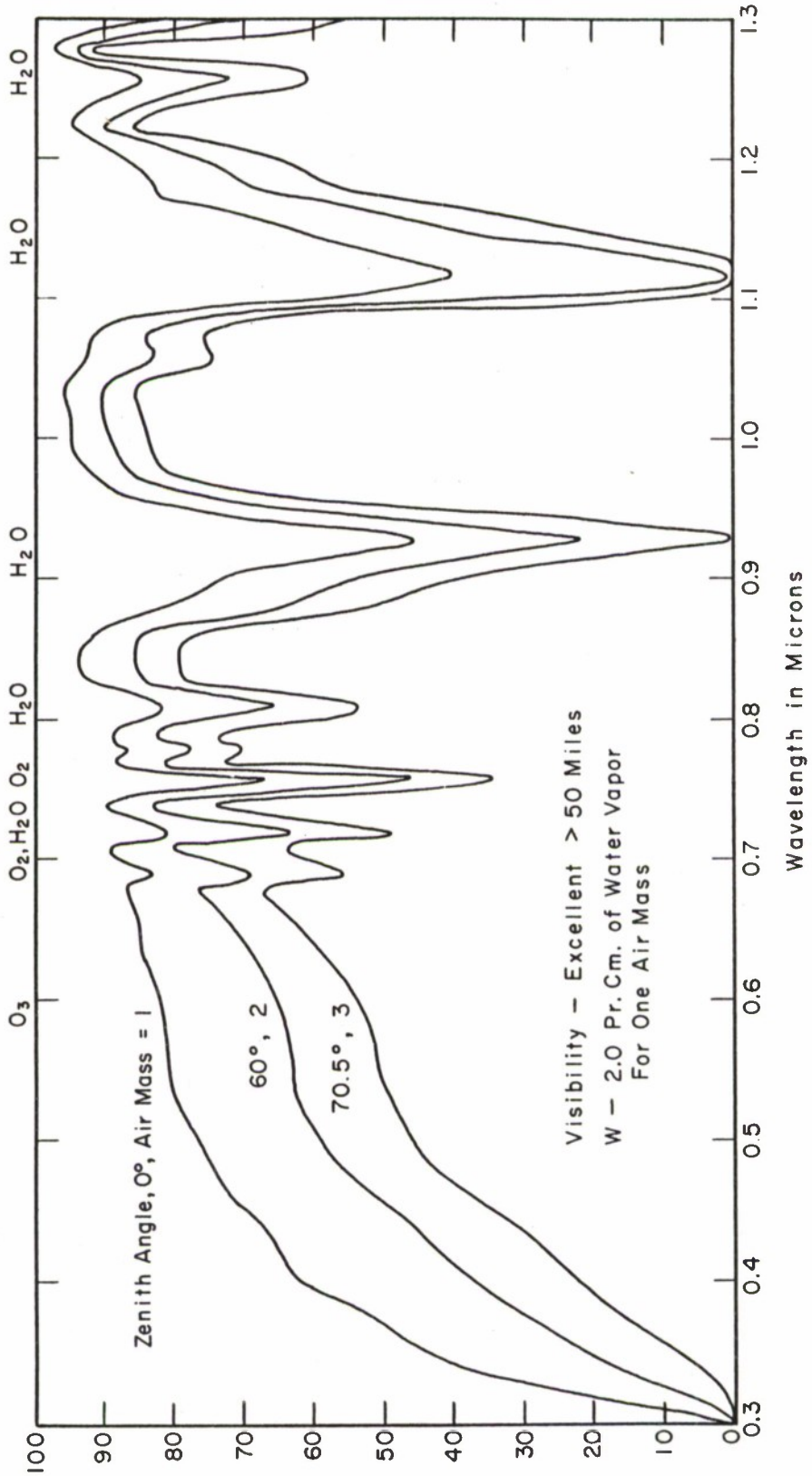

Figure 10. Atmospheric Transmission, 0.3 to 1.3 Microns

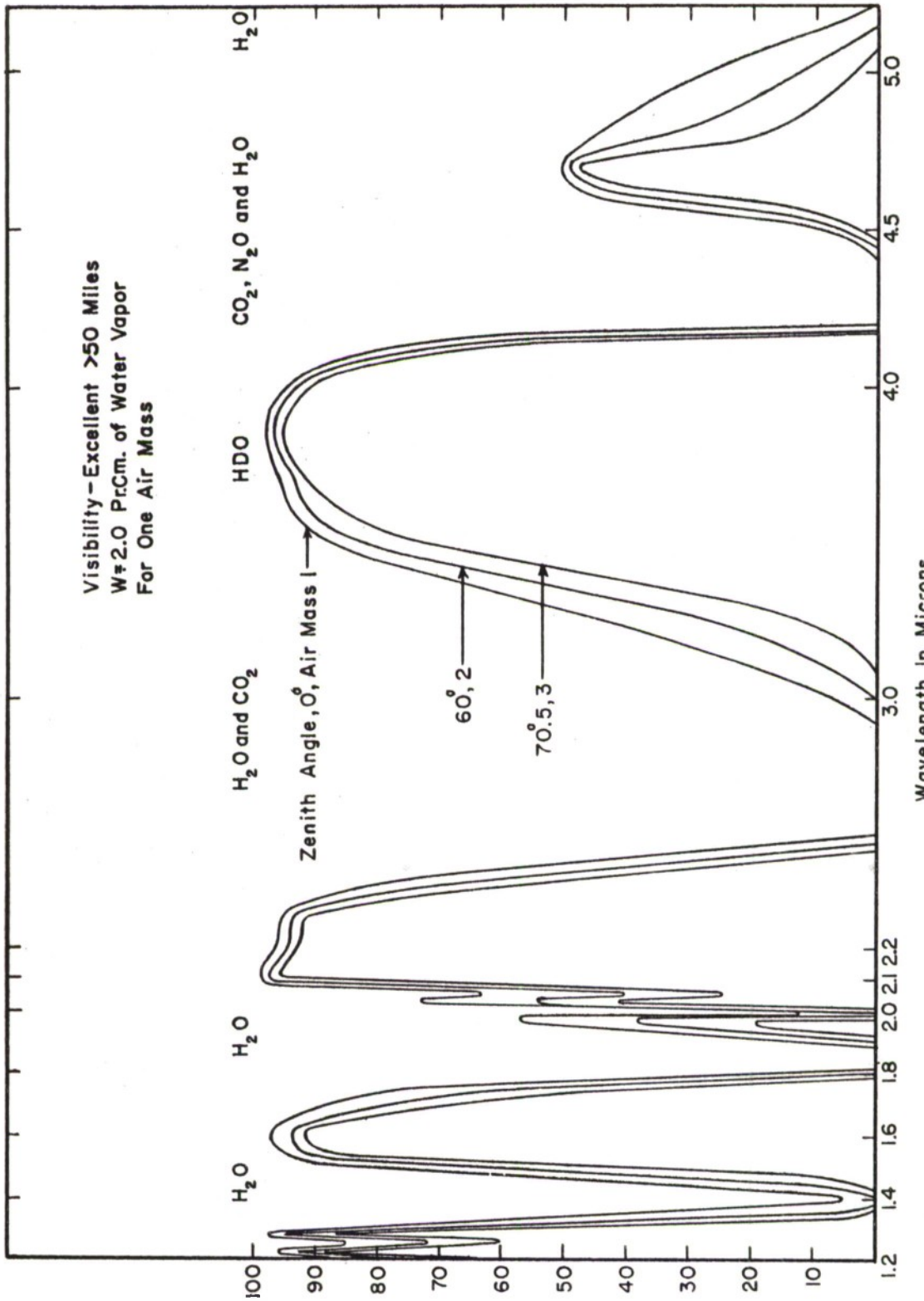

Figure 11. Atmospheric Transmission, 1.2 to 5.0 Microns

is an enormously complex subject which has occupied the attention of numerous specialists and astronomers for many years and is still not considered in the solved category, particularly since it is so sensitive to meteorological conditions.

The following facts should be kept in mind when considering the attenuation aspects of the wavelength regions presented in the figures relative to target observations.

1. The whole wavelength region from 0.3 to 5μ is full of thousands of sharp absorption lines due to H_2O, CO_2, N_2O, CH_2, O_2, O_3, CO and their isotopes. At low resolution these lines are smoothed out so that only the clustering in strong bands appears to give absorption.[4,5,6]

2. Absorption laws for gases follow an exponential form, e^{-kx}, only over infinitesimally small wavelength intervals which, in general, are almost impossible to resolve and even then are sensitive to pressure and temperature effects.

3. Scattering attenuation is due to small particle or molecular "Rayleigh" scattering, which is inversely proportional to the fourth power of wavelength, and "Mie" scattering of larger particles which is much less sensitive to wavelength. At very short wavelengths "Rayleigh" scattering alone can produce large attenuations.

4. Starting at about 2 microns in the infrared, the atmosphere becomes a strong emitter, for those wavelengths where it also absorbs, due to its own temperature. More will be said on this topic in another section.

---

4. "The Absorption Spectrum from 0.5 to 25 Microns of a 1000 Foot Atmospheric Path at Sea Level," H. W. Yates, NRL Report 5033, 27 September 1957.

5. "A Grating Map of the Solar Spectrum from 3.0 to 5.2 Microns," J. H. Shaw, R. M. Chapman, J. N. Howard, and M. L. Oxholm, Astrophysical Journal, 113:268, (1951).

6. "An Atlas of the Absorption of the Atmosphere from 5400 to 8520A," J. A. Curcio and G. L. Knestrick, NRL Report 4601, 23 August 1955.

5. This whole subject is so complex that it would be extremely desirable in any measurement program attempt to extrapolate back through the atmosphere to ascertain the spectral power characteristics of any target, to have separate attenuation measurements made at nearly the same time, using the same equipment and stars of known spectral characteristics.

I. The Seeing of Point Sources Through the Atmosphere

The effective angular diameter and intensity distribution of the telescopic image of a point source as it enters the slit of a spectroscopic system is one of the basic factors that influence the design, cost, and performance of the system.

The total effective size of such an image, and therefore the required slit width for maximum efficiency, is determined by a number of factors.

1. Deviation and Distortions Due to the Tracking System

This can be one of the largest sources of time-averaged smearing of the point source image, and in a radar-slaved telescope may amount to 1/2° or 1800 seconds of arc. An analysis of one of the consequences of this effect is discussed in Section II, C. For astronomical work the guiding and tracking can be kept below a fraction of a second of arc for long periods of time.

2. The Angular Diameter of the Point Source

The largest angular diameters of a point source such as a star or a 1 foot object at 50 miles are less than one second of arc. This contribution is negligible in most problems.

3. The Diffraction Disc or Circle of Confusion at the Objective

For a well ground and polished objective, the diameter of the circle of confusion approaches the diffraction disc, d, in size. The angular diameter of this disc is readily calculated: $d = \frac{2.44\lambda}{D}$ where λ

is the wavelength of light and D is the diameter of the objective. At 5000A , a good rule-of-thumb gives $d = \frac{8}{D}$ seconds of arc, where D is in inches. Obviously, for larger telescopes, atmospheric conditions, not the diffraction limit, determine image size.

4. Scattering in the Optics

Scattering of light, primarily caused by scratches and dust on the optical surfaces, contributes to the large faint aureole surrounding the image. According to Hosfeld,[7] this contribution can become an appreciable fraction of brightness at large distances from the image center, and cleaning of a 12-1/2 inch diameter refractor reduced the radius of aureole which could be detected photoelectrically from Altair from 25 minutes of arc down to 5 minutes of arc. At 12 seconds of arc radius, the intensity values were 0.45 and 0.05 per cent of total starlight before and after cleaning. In general, this factor should not contribute more than 1-3 seconds of arc to the total point source image diameter, i.e., the diameter that contains 98 per cent of the starlight, depending on the cleanliness of the optics.

5. Wavefront Deformations Caused by the Atmosphere

Atmospheric inhomogeneities and disturbances affect the distribution of light within a point source image in the focal plane of a telescope as a function of time.[8] The turbulent cells of refractive index different from that of the undisturbed atmosphere act as moving lenses passing in front of the telescope aperture.

The result is a distribution of light that causes motion of the image or its center of gravity, change in the size of the image or a brightness change sometimes defined as scintillation.

---

7. "Measurements of the Size of Stellar Images," Roger Hosfeld, Report No. AFCRC-TN-55-873, Ohio State University, June 1955.

8. "Investigations of Stellar Scintillation and the Behavior of Telescopic Images," G. Keller, W. M. Protheroe, P. E. Barnhardt and J. Galli, Report No. AFCRC TR 57-186; AD 117279, Ohio State University, December 1956.

The scintillation of stars is apparently due to a cellular structure of about 3 to 6 inches at about 5 to 15 km, with harmonic components of intensity which decrease roughly uniformly with frequency from 0.1 cps to 500 cps.[9] The equivalent sine-wave modulation of starlight increases in general with zenith angle and decreases with the diameter of the telescope aperture.[10,11] With a 36-inch diameter telescope under fair to good seeing conditions, the equivalent sine-wave modulation averages about 1-2 per cent in the zenith and increases with decreasing aperture to 5-10 per cent for a 3-inch aperture.

Wavefront deformations which occur closer to the objective if they are smaller than the telescope aperture cause size pulsations of the image which are generally limited to about 2-3.5 seconds of arc.

Larger deformations cause motion or damaging of the active image in the range of about 2-5 seconds between day and night for average sea level observing conditions.

These phenomena have frequency distributions which seem to be only slightly lower than for scintillation and have no great variation with wavelength in the visible.

6. Diffraction and Scattering by the Atmosphere

The aureoles around the sun and moon are examples of what happens less obviously to starlight. The contribution here is about 2-5 seconds between day and night for average sea level observing conditions.[7]

---

9. "The Scintillation of Starlight," A. H. Mikesell, Pub. U.S. Naval Obs., Second Series, 17:139, (1955).

10. "Fluctuations of Starlight 4. Preliminary Report on Stellar Scintillation," William M. Protheroe, Report No. AFCRC TR-54-115, Ohio State University, November 1954.

11. "Some Experiments on the Scintillation of Stars and Planets," M.S. Ellison and H. Seddon, Mon. Not. Roy. Astron. Soc., 112:73, (1952).

The following table summarizes the results and conclusions of the preceding discussion.

TABLE 3

CONTRIBUTIONS TO THE AVERAGE TOTAL SIZE OF STAR IMAGES AT NIGHT

	Estimated Range
1. Tracking System	0-1800 seconds arc.
2. Angular Diameter of Point Sources	0.02-0.8
3. Circle of Confusion (Diffraction Limited)	0.2-0.8
4. Scattering in the Optics	1-3
5. Wavefront Deformations in Atmosphere	2-8.5
6. Diffraction and Scattering in the Atmosphere	2-5

These sizes include 98 per cent of the starlight and only the wavefront deformations and tracking systems cause image displacement, the other factors would be expected to enlarge the image symmetrically. Further, the factors are not completely independent and variations in one may or may not be accompanied by variations in the others.

J. Man-Made Lighting

Artificial lights on the ground are scattered by fog and smog in the atmosphere so that a diffuse night sky background exceeding the limits estimated in Section I, F may be produced. We have not been able to make a definitive calculation of the amount of man-made background at Wallops Island since this would require a measurement with a sensitive photometer at the site.

At observatories near large industrial cities (i.e., Los Angeles, Columbus, Rochester, and Boston) it is found that the limiting magnitude

of an observable star with any instrument will usually run from one to four magnitudes greater than for more favorable locations depending on the visibility conditions and particular value of night sky background. At Mt. Wilson, a partial blackout of the City of Los Angeles reduced the diffuse sky background by almost three times and to near ideal conditions on days of little smog.[12] G. T. Keene[13] finds the limiting magnitude with a 12-inch telescope reduced by two at Rochester. This would indicate man-made scattered lighting 6 times that of night sky. In measuring the distant aureole of Jupiter, R. Hosfeld[14] found a limiting sky brightness of 19th magnitude per square second at Columbus, Ohio, while the average diffuse night sky background has a magnitude of 21.5.

Since Wallops Island is away from large industrial complexes, it would appear safe to assume that man-made lighting would be negligible if the telescope site is well removed from the launching site and other sources of very nearby lighting. Care should be taken to avoid bad fog and haze conditions, but these would disturb the transmission and seeing even more seriously than they would raise the background.

Note added in proof: Observation at the field test of March 3, 1959 conclusively indicated that man-made lighting at Wallops Island would be entirely negligible. During a test, all lights on the base were carefully shuttered. In any case, the total normal lighting on the isolated island is so small as to produce no sky background, with the possible exception of fog or haze near a camera within 100 yards of an exposed light.

---

12. J. B. Sidgwick, Amateur Astronomer's Handbook, Faber and Faber, London, 1955.
13. G. T. Keene, "Some Suggestions on Astrophotography," Sky and Telescope, January 1959.
14. R. Hosfeld, Sci. Report No. 2, Contract AF 19(604)-41, Ohio State University, June 1955.

SECTION II

STUDY OF THE SLIT SPECTROGRAPH WITH MULTIPLE DETECTORS

A. Properties of the Tracking System

A five-inch object at 100 miles subtends an angle of 7.9×10^{-7} radians, or 4.5×10^{-5} degrees, or 0.16 seconds of arc. Since this approaches the limit of resolution of the best telescopes as limited by atmospheric turbulence, for all practical purposes the source in the Lincoln experiments may be considered as an ideal point, not distinguishable by shape from any other star.

The night sky background behind the target emits a number of radiations from several sources which will be discussed in more detail as the main interest in this report. This background will serve to interfere with or obscure the attempt to measure the spectrum of the target emission. Since the total received background intensity at the telescope will increase directly as the instantaneous solid angular field of view, while the target intensity will be independent of the field as long as the target remains within the field, the best way of reducing or eliminating the night sky background interference is to narrow the field angle to the greatest possible degree. Unfortunately, this requires that the target be tracked to a very high accuracy.

It is not the purpose of our study to design or specify the tracking system, rather, it is to be assumed as one of the given elements of the situation. However, it is necessary to have knowledge of the properties of the tracking system in order to design the optimum telescope and spectrometer, and to estimate their performance and noise limitations in the presence of background.

It is to be assumed that some attempt will be made to estimate the average expected angular speed of the target object, and that tracker and telescope will be steadily advanced at this rate, leaving the tracking servo only the problems of correcting the smaller deviations from the expected trajectory. Thus the expected scatter in the prediction of the

trajectory angular rate is a parameter of interest, for the final rms tracking error may be a function of the speed difference which would have to be simultaneously corrected.

If there is a steady lag in the tracking position behind the target position, and the magnitude of this "fixed lag error" can be reliably predicted, a steady correction can be applied to the telescope so that it is on the average always centered on the target.

Finally there will be left the random component of the tracking error, so that the true target position will execute some sort of random path about the center of the telescope's field.

Certainly the parameter of tracking error which most vitally affects the spectrum equipment performance is the "rms displacement error," since it directly controls the size of angular field which must admit interfering background. In this connection the "rms" angular displacement is probably a better criterion for field limitation than the "peak" excursion, even if the latter could be reliably stated. The reason is that enlarging the field beyond the "rms" point may admit more background interference than new signal intensity, leading to a net loss. An exact calculation of the optimum field would require a detailed knowledge of the statistics of the error, but it is certainly more likely "rms" than "peak."

Some of the star discrimination schemes which are to be considered will involve chopping reticles over the field of view. In analyzing and predicting their performance, another property of the tracking system which will be important is the statistical distribution of velocity in the tracking pattern. The only thing which conveniently distinguishes the point target from a point star is its velocity. The chopping reticle would seek to convert the velocity difference into a frequency difference, then separate by frequency filtering. However, the random motion of the tracker will introduce random shifts in frequencies of target and stars. Thus, if the width of the jitter frequency spectrum is greater than the difference between target and star frequency, the discrimination method would be of little value.

To summarize, it would be helpful to know the following parameters of the tracking system:

1. The "rms" (and/or peak) tracking position error.
2. The probability distribution of angular position error.
3. The "rms" velocity of the random component of tracking error.
4. The probability distribution of angular velocty in tracking.
5. Sources and magnitudes of steady or "lag" errors.
6. The scatter in prediction of the target angular velocity.

The speed of the tracking error will be related in some way to the maximum angular speed of the tracking system, and perhaps to the expected scatter in the predicted target speed.

For the present, all our calculation will be based on an assumption of a 5 milliradian rms tracking error (radius).

B. Cell Noise Limitations - 1P21 Photomultiplier

If we assume for the moment that a telescope-spectrometer system of 100 per cent efficiency can be devised that will transmit all the energy in a narrow spectral band $\Delta\lambda$ passing through the telescope objective of area A_1, then the total energy in $\Delta\lambda$ collected on the photodetector is given by

$$\Delta W = \frac{W_\lambda}{R^2} \cdot A_1 \Delta\lambda = (SFD) \cdot A_1 \cdot \Delta\lambda \qquad (2)$$

Introducing the reference values

W_λ = 0.125 watts/steradian micron
R = 100 miles
SFD = 4.8×10^{-16} watts/sq cm-micron
(spectral flux density at telescope from target)

The 1P21 photomultiplier will almost surely be the most sensitive, readily available detector for all wavelengths up to its work function

threshold at about 5700 angstroms. It has been demonstrated that it is possible to manufacture this tube with sufficiently low leakage currents and use it with a sufficiently steady power supply so that the only noise limitation is the fluctuation in the dark thermionic emission. Under these conditions, the "noise equivalent power," NEP, or threshold of the 1P21 tube is given by

$$(\text{NEP}) = \frac{hc}{\lambda_\mu \, q_\lambda} \left[2 n_d \, A \, \Delta f\right]^{\frac{1}{2}} \qquad (3)$$

$hc \approx 2.0 \times 10^{-19}$ joule-micron.

where λ_μ = wavelength of signal in microns (reference 0.5_μ).
$q\lambda$ = quantum efficiency, electrons/photon (~ 0.20).
n_d = thermionic current = 60,000 electrons/cm^2 sec. @ 300°K.
A = area of cathode (~ 1.5 cm^2 for 1P21 type).

In order to make this or any other noise computation, it is necessary to make some assumption about the observation bandwidth. This will be fundamentally limited only by the number of spectral observations it is desired to make per second. As a reference value, we will assume 6 spectrum determinations per second; thus, each detector will have a response time, T = 1/6 sec., and the effective bandwidth of the system will be

$$\Delta f = \frac{1}{2f} \approx 3 \text{ cps.} \qquad (4)$$

This bandwidth will be adequate for indicating the growth and decay of the "gaslight" curve of Figure 1 (see the time scale) if we assume that there is a separate detector for each spectral band which it is desired to resolve. If it should be considered economically necessary to use fewer separate detectors and time-share them in order to cover more spectral bands, some sacrifice would have to be made in either noise, bandwidth or number of observations per second. It should further be pointed out in this connection that in the initial stages of a weak light situation such as this, it is fundamentally wasteful of light energy not to collect every spectral wavelength at all times in some detector. Therefore, it would seem better to

consider widening the spectral bandwidth with the consequent improvement in signal and S/N than to leave any gaps in the spectrum, even if the gaps should be picked up later by a time-sharing method.

Our recommendation is to always operate with adjacent spectral bands with no gaps, providing the necessary number of detectors, and data handling and recording capacity. If one exceeds the available recording capacity, the spectral bands should be widened. This would still convey all the information the recording system can accommodate.

Inserting the reference values we obtain for the NEP of 1P21 at 300 degrees Kelvin:

$$NEP = 1.5 \times 10^{-15} \text{ watts} \qquad (5)$$

In order that the energy ΔW collected by the telescope-spectrometer exceed this NEP, the requirement is that $A_1 \Delta\lambda$ be larger than

$$(A_1 \Delta\lambda)_{S/N = 1} = \frac{NEP}{SFD} = 3.1 \text{ cm}^2\text{-micron}$$

Example: if $\Delta\lambda$ = 10 ang = $10^{-3}\mu$, then A_1 = 3100 cm^2.

The thermionic dark current and fluctuations can be further reduced by cooling the tube below 300°K. Further investigation of existing data would be required to determine just how much improvement could be thus obtained, for one might soon reach a point where cosmic electrons or other noise sources become predominant. Since the external background fluctuations are likely to be a more serious source of noise interference, it is doubtful whether the inconvenience of cooling would be justified.

C. Required Size of Spectral Dispersing Element

In the preceding sections a spectrometer of 100 per cent light collecting efficiency has been assumed. Before entering the discussion of the night sky background, it is of interest to investigate the required size of grating or prism to provide this 100 per cent efficiency. It will be found that a

rather large dispersing element will be required unless we can devise a highly efficient image dissection method to match the telescope field shape to the spectrometer entrance slit shape.

This problem can be considered in relation to Figure 12.

F_1, F_2	Focal length of telescope and spectrometer, respectively.
D_1, D_2	Diameter of telescope and spectrometer, respectively.
α	Twice the "rms" tracking error, or field of view.
$\Delta\lambda$	Spectral band width to be resolved.
$d\theta/d\lambda$	Angular dispersion of the dispersing element.

It is assumed that the spectrometer is symmetrical between collimator and focus, with entrance and exit slits equal. No other arrangement can collect more light.

The physical linear dimension of the telescope image (limited by an aperture) is $F_1\alpha$. The width of the entrance slit is $F_2 \frac{d\theta}{d\lambda} \Delta\lambda$. If the spectrometer is to collect all the light, these must be equal.

$$F_1 \alpha = F_2 \frac{d\theta}{d\lambda} \Delta\lambda$$

Since the focal ration F/D of telescope and spectrometer must be equal,

$$\frac{F_1}{D_1} = \frac{F_2}{D_2} \qquad (6)$$

Therefore, the size of the dispersing element relative to the size of the telescope aperture is given by

$$\frac{D_2}{D_1} = \frac{\alpha / \Delta\lambda}{d\theta / d\lambda}$$

This ratio depends only on the "rms" tracking error, the desired spectral resolution, and the angular dispersion, which is an inherent property of the

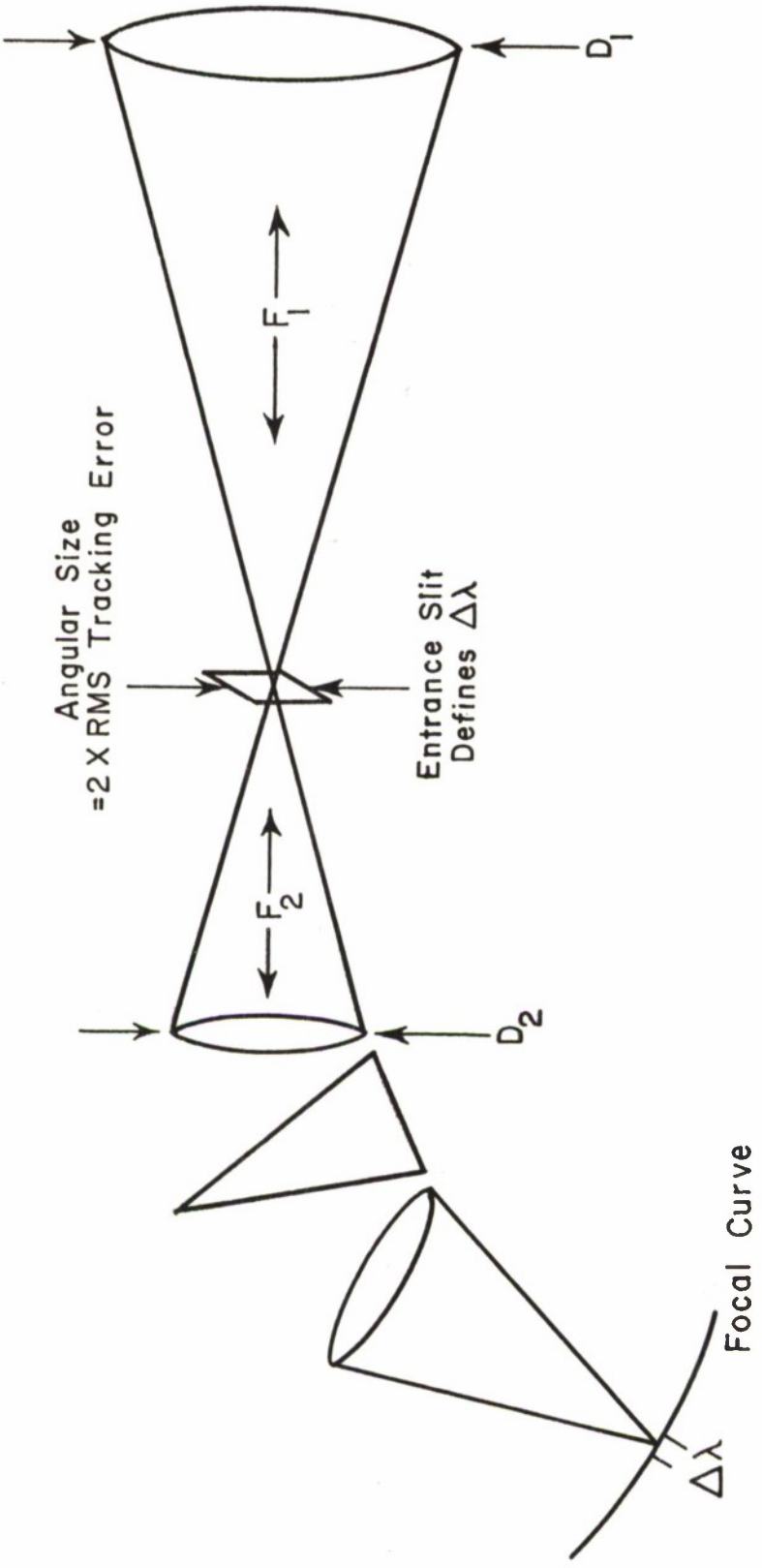

Figure 12. Factors Determining Size of Dispersion Element

dispersing device. Two cases will be considered, a grating of 15,000 lines per inch, and a flint glass prism. We assume that the field of view is 10 milliradians; the spectral bandwidth 10^{-3} microns (10 angstroms).

For the grating, the angular dispersion is

$$\frac{d\theta}{d\lambda} = \frac{m}{a \cos\theta}$$

m = order of interference (assume 1)

a = line spacing = 1.7 microns for 15,000 line/in.

Assume $\cos\theta \approx 1$

Thus $\frac{d\theta}{d\lambda} \approx$ 0.6 radians/micron

and $\frac{D_2}{D_1} \approx$ 16 !

For the prism,

$$\frac{d\theta}{d\lambda} = 2 (\tan A/2)\, dn/d\lambda$$

and for a 60 degree prism, $2 \tan A/2 = 1.15$

at 5000 angstroms, $\frac{dn}{d\lambda}$ = 0.2 for flint glass
0.08 for quartz

Thus the dispersion is only a little better than 1/3 of the grating, and all other quantities being the same, the flint glass prism requires nearly three times the size of the above grating.

It is possible to obtain another factor of two with finer gratings, 30,000 lines per inch being fairly common, and there is a gain in dispersion by operating at higher orders. At higher orders it becomes more difficult to design a spectrograph to cover a wide range, and order separation by filters, or otherwise, sometimes becomes difficult.

In addition to their lower dispersion, prisms lead to more difficulties with curved focal plane, and the dispersion and resolution vary with wavelength.

Other than obtaining more precise tracking, thus reducing α , or relaxing the requirement for narrow band $\Delta\lambda$, about the only recourse left that maintains 100 per cent optical efficiency is the use of "image dissection." The basic problem is that the image of the field of view is too wide for the narrow spectrometer slit, though the spectrometer could pass considerably more light by lengthening the slit in the other direction. Therefore, if the telescope image were sliced into parts, and the light were retransported to form a long narrow slit, one would reduce the grating size requirement exactly by the number of slices, N, into which the image were divided. Thus with image dissection into N parts, the complete formula for grating size becomes

$$\frac{D_2}{D_1} = \frac{\alpha/\Delta\lambda}{N\,(d\theta/d\lambda)} \qquad (7)$$

The use of fiber optics, or the "Fiberscope" of American Optical Co., offers an attractive way to produce "image dissection of high optical efficiency." (See also the appendix to Strong's "Concepts of Classical Optics".) There are also some other methods of image dissection based on simple arrangements of mirrors.

D. Statistical Fluctuations in the Steady Night Background

The total flux received from the night sky by our telescope-detector will be

$$W_B = B_N \cdot A_1 \cdot \Delta\lambda \cdot \Omega$$

with equation (2) for the target flux, we see that the diffuse background contains the additional factor $\Omega = \pi/4\ \alpha^2$, the solid angular field of view of the telescope slit. Therefore, reduction of the tracking error and the field of view can greatly reduce the background relative to the signal.

Even if the diffuse background is steady, or can be made so by subtracting a comparison run, the background flux still generates noise because of its inherent statistical (quantum)fluctuations. The signal to noise is given by

$$S/N = \frac{N_S}{\sqrt{N_S + N_B + N_T}}$$

Where N_S, N_B, and N_T are the number of electrons ejected by the cathode within the time constant of the equipment by signal, background, and thermionic emission, respectively.

$$N_S = (SFD)\ A_1\ \Delta\lambda\ \gamma\ q\ T$$

$$N_B = B_N\ A_1\ \Delta\lambda\ \Omega\ \gamma\ q\ T$$

$$N_T = n_d\ A\ T$$

where γ = the number of photons per joule $\frac{\lambda}{hc} = \frac{\lambda_\mu}{2} \times 10^{19}$

For the assumed 1P21, with T = 1/6 sec., N_T = 15,000, $\sqrt{N_T}$ = 122. Thus in the absence of background (N_B = 0), $N_S << N_T$ at threshold. This is the threshold indicated in equation (3). The background will begin to affect the threshold significantly when $N_B = N_T$, which sets a condition on the allowable solid angle of view Ω, when the background spectral brightness B_N is known.

$$\Omega = \frac{n_d A}{B_N\ A_1\ \Delta\lambda\ \gamma\ q} \qquad \text{for } N_B = N_T$$

if the aperture and band are chosen to match the thermionic threshold alone,

$$A_1\ \Delta\lambda = \frac{NEP}{SFD} = 3.1\ \text{cm.}^2\ \text{-}\mu$$

then the critical value of Ω can be written,

$$\Omega = \frac{(SFD)}{B_N} N_T^{\frac{1}{2}} = 1.3 \times 10^{-4} \text{ steradians}$$

For the estimated 5 mil tracking radius, $\Omega = 0.8 \times 10^{-4}$ steradian, so for the estimated target and background strength, the situation is not too bad.

When both thermionic and background emission are acting together to produce noise, a more general NEP should be written

$$(NEP)^1 = \frac{1}{\gamma q f} (N_B + N_T)^{\frac{1}{2}}$$

In order to exhibit the significance of the available choices, it is perhaps more instructive to calculate the "noise equivalent spectral flux density,"

$$(NESPD) = \frac{(NEP)^1}{A_1 \Delta \lambda} = \frac{1}{A_1 \Delta \lambda \gamma q \sqrt{T}} (B_N \Omega A_1 \Delta \lambda \gamma q + n_d A)^{\frac{1}{2}}$$

This equation is plotted in the solid line of Figure 13. The estimated value of target SFD which was chosen to be detected at the arbitrary limits of 100,000 and 250,000 feet of the trajectory is indicated. One can always improve the threshold by increasing $A_1 \Delta \lambda$, the aperture or the spectral bandwidth. At first this improvement is directly proportional to $A_1 \Delta \lambda$ until the background flux becomes dominant, depending on $B_N \Omega$, after which the improvement is more gradual, as the square root of $A_1 \Delta \lambda$. If $B_N \Omega$ can be improved, as by better night sky conditions or better tracking, the threshold shifts to curve B. If the thermionic emission $n_d A$ can be reduced, as by cooling or smaller cathode area, the threshold shifts to curve C.

With the estimated values assumed for every parameter, the required value of $A_1 \Delta \lambda$ is about 4 $cm.^2$-micron.

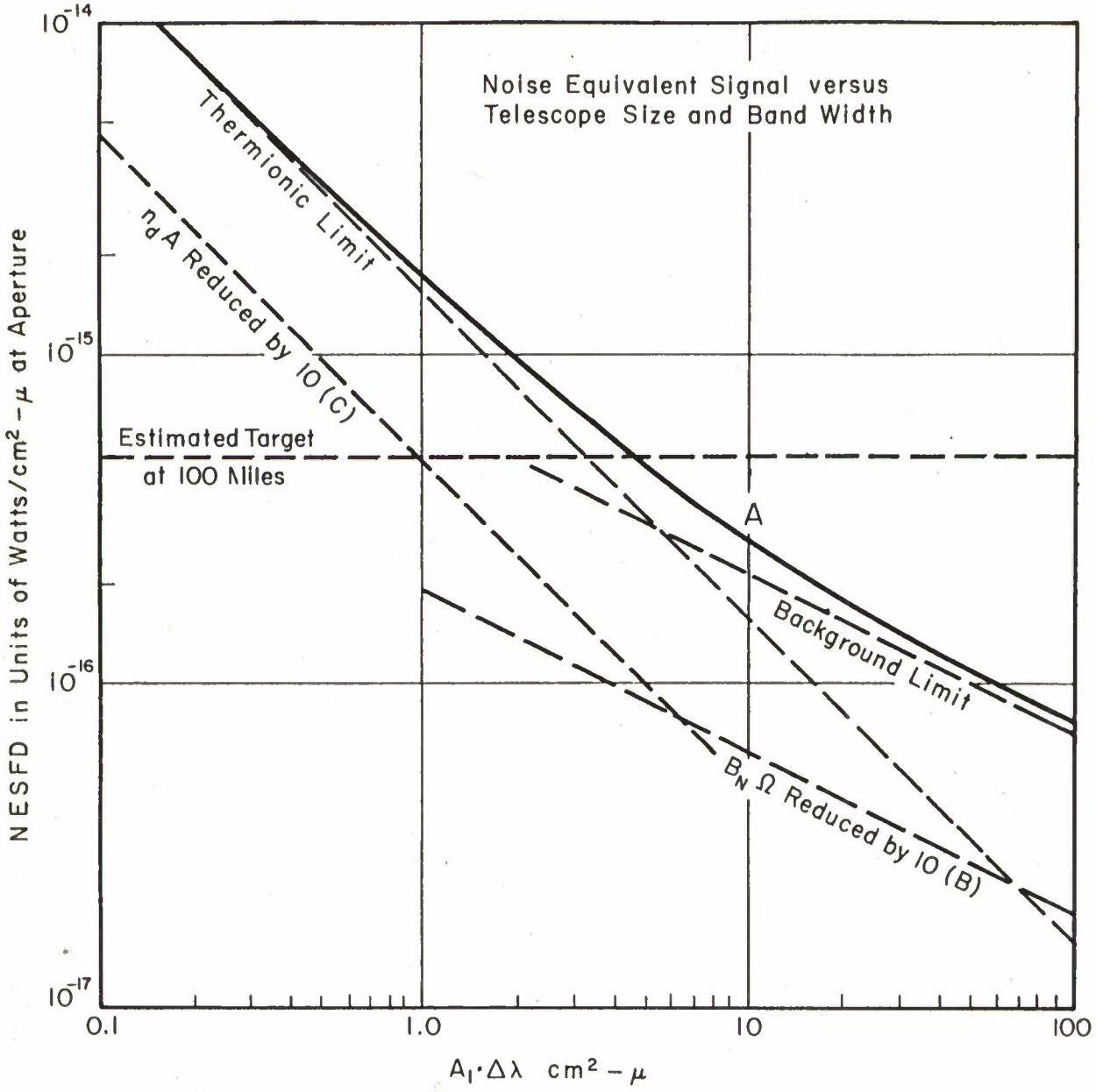

Figure 13. Noise Equivalent Signal

E. Estimate of Trajectory Speed, Time of Star Passage, and Power Spectrum

Since the telescope field is assumed to remain fixed on the target, the apparent speed of stars relative to the telescope field is the same as the real angular speed of the target relative to the stars. This depends on the point of observation and the trajectory, as shown in Figure 1, assuming that the trajectory is a straight line. In general, the target angular speed is given by

$$\frac{dE}{dt} = \frac{v}{B} \cos^2 E$$

where v is the target velocity B is the baseline.

$$\approx 0.039 \text{ radians/sec} \approx 2.24 \text{ degrees/sec.}$$
(reference value)

If for simplicity we assume that the field of view is a square 0.01 radians on a side, it is clear that the time for the passage of a single star is about 1/4 second. See a single star pulse in Figure 14. The amplitude of the square pulse, A_m, is left arbitrary for the moment. The energy in the pulse is proportional to $A_m^2 \delta t$. The Fourier spectrum of a square pulse is well known (see any table of Fourier Transforms).

$$g(f) = \int_{-\infty}^{\infty} a(t) e^{i2\pi ft} dt = \frac{A_m \sin(\pi f \delta t)}{\pi f}$$

The energy spectrum is

$$E(f)\, df = g^2(f)\, df = \frac{A_m^2 \sin^2(\pi f \delta t)}{(\pi f)^2}\, df$$

and

$$\int_{-\infty}^{\infty} g^2(f) df = \text{total energy} = A_m^2 \delta t = \int_{-\infty}^{\infty} a^2(t)\, dt$$

Now if many such stars arrive at the field of view at random intervals, but of average frequency N_m per second, the power spectrum is simply N_m times the energy in a single pulse

$$P_m(f) = N_m g^2(f) = N_m A_m^2 \frac{\sin^2(\pi f \delta t)}{(\pi f)^2}$$

If there are several discrete sets of such random pulses, all of the same width δ t, but each set with a specified amplitude A_m and average frequency of arrival N_m, the power spectrum is again simply additive.

$$P(f) = (\Sigma_m N_m A_m^2) \frac{\sin^2(\pi f \delta t)}{(\pi f)^2}$$

and the average power in the whole spectrum is

$$\int_{-\infty}^{\infty} P(f)\, df = (\Sigma_m N_m A_m^2)\ \delta t$$

or the effective rms amplitude is

$$A_{rms} = \sqrt{(\Sigma_m N_m A_m^2)\ \delta t}$$

The power spectrum is illustrated in Figure 14. The peak value at $f = o$ is $(\Sigma_m N_m A_m^2) \times (\delta t)^2$. Zeros, or minima occur at $f = \frac{n}{\delta t} = 4n$ cps ($n = \pm 1, \pm 2, \pm 3 \ldots$). The half-power point occurs at $f = \pm \frac{1}{2\delta t}$, or the full width between half-maxima is $\Delta f = \frac{1}{\delta t} = 4$ cps. The first secondary maximum has the value 4.4 per cent of the peak, next 1.6 per cent, next 0.8 per cent, and so on.

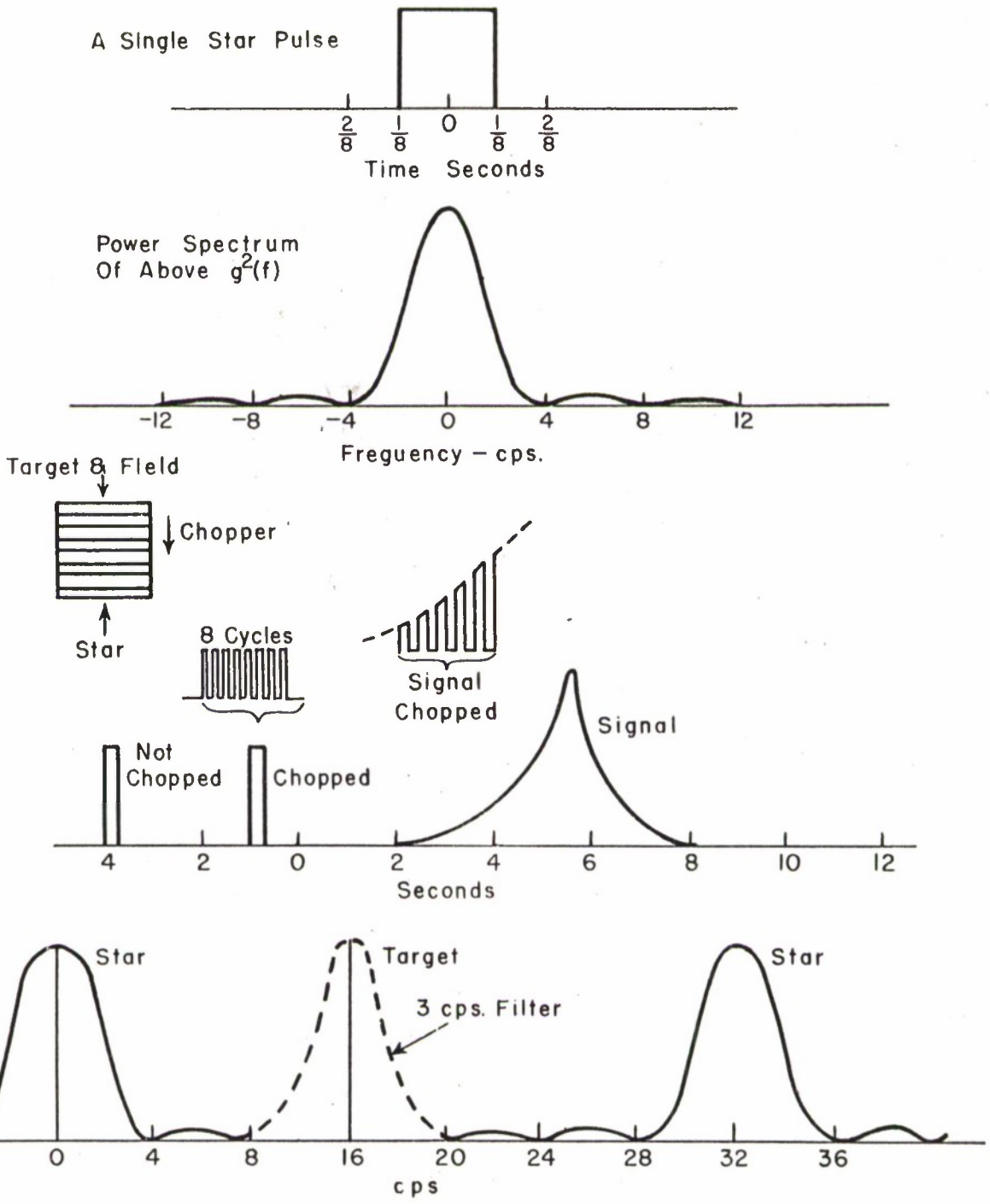

Figure 14. Star Pulse Shapes and Frequency Spectra

F. Evaluation of the Venetian Blind Clutter-Rejection Chopper

It has been shown that the brighter star pulses, at rare intervals, contribute the major portion of the interfering star noise power. Therefore, it is of advantage when evaluating their effect to change the point of view from the statistical analysis to the consideration of the elimination of single star pulses.

One method would be simply to identify and subtract the star pulses. This is not as difficult as it sounds because of the relative rarity of the brighter stars. The identification might be made by plotting the trajectory on the star chart, and by making a comparison run with the photometer equipment over the same trajectory without target shortly after the measurement run. These methods would be used in conjunction with any available methods of "discriminating" or reducing the amplitude of the star pulses.

A "Venetian blind" chopper was suggested by R.V. Meyer as a feasible method of discrimination. This is illustrated in Figure 14, and consists of chopper blades across the field of view moving in direction along the trajectory, which is presumed to be roughly predictable. This scheme is based on the idea that the principal distinction between target and star is the difference in angular velocities, therefore, they will be chopped at different frequencies, and the target frequency can be selected by filtering. This scheme has been analyzed and some general quantitative conclusions drawn as to its discrimination effectiveness.

The given parameters are:

$\dot{\theta}_o$, the angular target speed (relative to the sky).
α , the diameter of the field of view.

These determine the time duration of a star pulse, $\delta t = \alpha/\dot{\theta}_o$
Subject to design choice are:

N, the number of chopper cycles instantaneously in the field.
$\dot{\theta}_c$, the chopper angular speed (relative to the field image).

Then the frequencies of the chopped target and star signals are

$$f_t = \frac{N}{\alpha}\dot{\theta}_c = \left(\frac{N}{\delta t}\right)\left(\frac{\dot{\theta}_c}{\dot{\theta}_o}\right) \tag{1}$$

$$f_s = \frac{N}{\alpha}\left(\dot{\theta}_o + \dot{\theta}_c\right) = \left(\frac{N}{\delta t}\right)\left(1 + \frac{\dot{\theta}_c}{\dot{\theta}_o}\right) \tag{2}$$

$$f_t - f_s = \frac{N}{\alpha}\dot{\theta}_o = \frac{N}{\delta t} \tag{3}$$

If these frequencies were sharp and discrete, and the filter had sufficiently steep cutoff, a very large discrimination of the star pulse could be achieved. This possibility is limited by the frequency spread of the star frequency caused by two effects: (1) the natural spread $\Delta f_1 \approx \frac{1}{\delta t}$ due to the finite duration of the star pulse in time, and (2) the extra frequency shifts added by the velocity error $\dot{\theta}_e$ of the tracking system, with $\Delta f_2 \approx \frac{N}{\delta t}\frac{\dot{\theta}_e}{\dot{\theta}_o}$. The ratio of output star amplitude to input star amplitude has been roughly estimated for each of these effects in turn.

For the natural spread, Δf_1, considered alone:

$$\frac{A_o}{A_i} \approx \left\{\frac{1}{40N^2}\ \frac{\delta t}{T}\right\}^{\frac{1}{2}} \tag{4}$$

For spread Δf_2 due to tracking error

$$\frac{A_o}{A_i} \approx \left\{\frac{\Delta\dot{\theta}_e}{\dot{\theta}_o}\cdot\frac{1}{2N}\cdot\frac{\delta t}{T}\right\} \tag{5}$$

T is the response time of the system, which determines the width $\Delta f_3 = \frac{1}{2T}$ of the discrimination filter which can be used. $\Delta\dot{\theta}_e$ is the "rms" value

of the component in the chopping direction of the angular velocity of the tracking error. The details of the analysis will not be given, only some general comments and conclusions:

1. If T is greater than δt there is a smoothing by integration of the star pulse, which reduces its amplitude by $\sqrt{\delta t/T}$ without chopping. Therefore, only the other factors in (4) and (5) can be said to be contributed directly as a result of chopping.

2. It is important to get the target frequency, f_t, well removed from zero in order to avoid passing additional star signals into the filter from the DC component of the star pulse. If $|\dot{\theta}_c|$ is 3 or more times $\dot{\theta}_o$, this is sufficient for this purpose, and the limiting discrimination listed above is reached.

3. Taking $\dot{\theta}_o$, $\dot{\theta}_c$, δt, T as given quantities, N as subject to choice, there is a critical value of N at

$$N_{crit} \approx \frac{1}{20} \frac{\theta_o}{\Delta \dot{\theta}_e}$$

where the filtered pulse energy from the two effects is equal. Increase of N above this point will have a less pronounced effect on the pulse amplitude.

4. The quality of the overall optical system must be able to produce instantaneous star (or target) images smaller than the chopper blade size. Therefore, for economical reasons N should not be made too large.

5. The dependence on the "rms" tracking velocity error is shown in (5). This result was derived on the assumption that the distribution of velocity errors had the shape

$$n(\dot{\theta}_e) = \frac{\Delta \dot{\theta}_e}{\dot{\theta}_e^2 + (\Delta \dot{\theta}_e)^2}$$

This has the property of falling off 6db/octave at the wings.

G. Summary of Performance of the Slit Spectrograph

The chief advantage of the slit spectrograph is that it effectively excludes all sky background, diffuse and star, except for the angular dimensions of the stellar image, which is limited by the telescope definition, the atmospheric seeing, and the tracking errors.

Assuming our crude estimates for target spectral intensity at 250,000 feet altitude, or 1 per cent peak intensity, it has been estimated that a 24-inch telescope is required to collect enough energy from a 10 angstrom band to reach the 1P21 threshold in 1/6 second integration time.

The diffuse night sky background in a 10 angstrom band from a sky angle of 10 milliradian square is approximately 90 times the above minimum target intensity, but its fluctuations just equal the target, or the thermionic noise threshold for this 1P21 system.

The size of the tracking error directly affects several factors of considerable importance to the performance:

1. The required area of dispersion element through equation (7). Unless this requirement is avoided through some form of image dissection, any tracking error larger than 1 milliradian will lead to excessively large grating requirements.
2. Both the frequency of occurrence and amplitude of the clutter from the fixed stars in the sky are reduced with finer tracking and smaller slit. Below 0.1 milliradian (20 secs.) tracking, the star interference would probably not be troublesome.
3. For large tracking error, or weaker targets than the above, the diffuse background fluctuations can exceed thermionic noise, with degradation of threshold sensitivity.

The principal disadvantage of the slit spectrograph is the size, expense, and complexity of instrument required to be tracked to such high precision. The most convenient arrangement is probably the classical Coude, where only the large telescope has to be pointed, and the spectrograph is mounted fixed in a pit below the Coude axis.

The limited time of target emission renders it impractical to use time-sharing scanning modes of operating one or a few detectors, and leads to a requirement for hundreds of detectors and duplicating amplifiers and recording channels. This is cumbersome and expensive. For this reason it would be desirable if the tracked slit spectrograph could be restricted to a few channels for detailed, continuous, and repeated study of only a few major lines or features of the emission.

For these reasons there is a need for a simpler, more versatile, "back-up" instrument suitable for recording the complete spectrum for qualitative evaluation, even if at considerably reduced sensitivity so that only a single exposure at the peak emission of each re-entry test could be obtained.

Therefore, in the following sections we will review briefly the performance equations for an objective streak spectrograph-telescope with a prism or grating before the objective.

SECTION III

SLITLESS OBJECTIVE SPECTROGRAPH

A. The Cassegrain Telescope-Objective Spectrograph

For a versatile instrument of moderate complexity, cost, and sensitivity, we have considered a Cassegrain mounting with objective prism. Although this telescope would not compete with the focal ratio which can be achieved with the Schmidt design, it is felt that the advantages of a flat and accessible field permitting the ready interchange of any one of a group of detecting systems is more than worth the loss in focal length or focal ratio. Further, with longer focal length, smaller dispersions and prism angles can be used, with less glass absorption path. This application requires a field of less than one degree, while the Schmidt is indicated for fields of tens of degrees.

The following parameters appear to lead to a system useful for the intended application:

Aperture: 12-1/2 inches.
Focal length: 100 inches.
Focal ratio: f/8.
Dispersion: 15 degree flint glass prism, $d\theta/d\lambda$ approx. 0.05 rad./micron.
Length of spectrum: 1.5 inches per 3000 angstroms, or about 0.125 mm per 10 angstroms.
Angular field: about 1 degree
Image quality and atmospheric seeing: 5 secs. of arc, which gives a monochromatic image width of 0.06 mm.

The focal plane would be provided with the possibility of interchanging any of the following detectors:

1. Image Orthicon with several intensifier stages.
2. Lallemand type photoelectric film intensifier.
3. Photographic film or plate.
4. 30-element linear array of PbS cells (IR Industries).

Type 1 has a resolution of about 0.08 mm, types 2 and 3 about 0.02 mm.

Thus the focal length, dispersion, and image quality have been chosen so that the 10 angstrom band covers just slightly more than one resolution element of the Orthicon and perhaps twice the size of the stellar image, neglecting tracking smearing. The energy collected from a point source at infinity depends only on the telescopic aperture, but the most efficient exposure of an imaging detector requires that one spectral band be concentrated on only a few detector elements.

a. Estimated Target Intensity

Watts in stationary image: $= (SFD)\ A \cdot \Delta\lambda$

$= 3.4 \times 10^{-14}$ watts

taking SFD at the peak intensity of 4.8×10^{-14} watt/cm$^2\mu$. This is equal to about 85,000 photons/second in the image of size 0.06 by 0.12 mm. Since the target remains above its half-intensity points about 1.5 seconds, this number is also about the total photon number obtainable in this 1.5 seconds. This is also about the number required to expose fast film to 0.6 density.

Therefore, it is clear that the objective spectrograph has not greatly reduced the requirement for tracking precision, since the target must be held to 5 seconds of arc for 1.5 seconds time in order to avoid smearing this photon concentration. The Lallemand device has been proven to be some 50 times more sensitive than fast film, so that some tracking smear is permissible. The guidance problem will be discussed later.

b. Estimated Diffuse Background Intensity

$$\frac{A}{F^2} \quad B_N \ d\lambda \approx \quad 2 \times 10^{-13} \ \text{watts/cm}^2.$$

Diffuse = 360 photons/second in 0.06 x 0.12 mm image size. On the average, the point stars' contribution to the background can be estimated to be 50 per cent of the above calculation for the diffuse background. This is

because the rapid motion of the stars relative to the telescope tends to smear them out as if they were diffuse, and accurate measurements have shown that the stars average 50 per cent of the diffuse brightness. A factor of 5 to 10 times less than this average value for both diffuse and stars can be obtained if it is possible to fire the target in favorable portions of the sky, away from the Galaxy and away from the zodiacal light.

The sky background per cm^2 on the focal plane is much larger in the case of the objective prism than in the case of the slit spectrograph because background is accumulated from an angle of sky equivalent to the length of spectrum, rather than just over the angular width of the slit. However, this is not so readily apparent from our calculations since we have assumed 5 second pointing accuracy for the objective spectrograph, but 2000 second pointing accuracy for the slit spectrograph. For background purposes the slit spectrograph requires only coarse pointing, although reasonable grating sizes require somewhat finer pointing. We have already seen that for sufficient concentration of photons on the detector the objective spectrograph requires extreme pointing precision. This precision is also adequate to reduce the background to a harmless value, if the shutter carefully admits background only while the target is intense.

B. Tracking the Objective Spectrograph

It appears that the objective spectrograph requires even higher tracking precision than the slit spectrograph. However, the objective spectrograph has a field of over one-half degree within which the target might be initially located; it is only that it must be held stationary once exposure is started. This raises the question whether some form of highly smoothed rate advance from the radar and optical tracker signals might be used once the exposure was initiated.

While approaching its peak emission, the target might be tracked with the full radar signals with one-half degree accuracy. Just before exposure is initiated, the radar would be disconnected, and the telescope mount's positioning motors would be advanced very smoothly from the best target velocity signals available. In this way it might be possible to hold the target to within 10 or 20 seconds of its original position for an exposure time of as much as 1.5 seconds.

C. Four Telescope Array

For versatility and for recording spectra in several spectral regions, it is suggested that four 12-1/2 inch telescopes could be mounted on a single gun mount. This was one reason for choosing this smaller aperture telescope, which is commonly available at moderate cost, and light in weight. One of the four previously listed detection systems could be used on each of these telescopes.

D. Stationary Objective Spectrograph

For bright meteors, astronomers have used stationary meteor streak spectrographs, since it is not possible to predict the velocity. For the Wallops Island re-entry objects, this procedure would avoid the expenses and complexity of a highly accurate telescope guidance servo, but it would be very disadvantageous with respect to intensity of the target spectrum and the relative interfering intensity of the background.

The flux density (watts/cm^2) in the target image is given by

$$\frac{(SFD)\ A}{\epsilon\, F^2 \frac{(d\theta/d\lambda)}{(d\theta/dt)}}$$

where (SFD) is the target spectral flux density at the telescope aperture,

A is the telescope aperture, F is its focal length,

ϵ is the angular image size limited by seeing and aberrations (20 seconds).

$d\theta/d\lambda$ is the angular dispersion of the spectrograph.

$d\theta/dt$ is the angular velocity of the target in the sky.

The corresponding flux density in the background is given by

$$\frac{A}{F^2} \int B_N \, d\lambda$$

since in a slitless spectrograph the entire spectrum is accumulated at each point of the film. In addition, the background is accumulated during the entire time the shutter is open, while the target is exposed only for the time it requires to traverse one spot diameter, $\epsilon \div d\theta/dt$, about 1/360 second under the average conditions.

To summarize, the relative background intensity in a stationary meteor streak spectrograph for this application is 300,000 times the background for an accurately tracked slit spectrograph, and 1000 times the background for an accurately tracked slitless spectrograph, of otherwise equivalent specifications.

Using estimates previously given in this report, and f/1 optics, it is estimated that it would take at least 20 seconds for the background to expose fast photographic film to 0.6 density. Lallemand plates are 50 times as fast, or would take 0.4 seconds.

For the target to produce the same exposure would require SFD of 6.6×10^{-12} watts/cm^{2}micron, or about 150 times the present estimates for the gaslight. It is possible that after intense ablation has started, these intensities may be reached.

The target spectrum intensity can be increased by any method which slows down the velocity of the target across the plate. This would require using all available information as to the location and speed of the target to advance the telescope or the photographic plate approximately with the target, even if it were not precisely tracked. This is, of course, no more than the readoption of partial tracking.

The background might be reduced, but the target intensity not improved, by adding a movable slotted plate in front of the emulsion. Assume the target moves 8 degrees in 3 seconds, and that there are 8 slots 1/8th degree wide and 1 degree apart, parallel to the dispersion. The camera is kept stationary, but either the detector or the slotted plate is moved at the rate of 1 degree per second. Thus the slots are exposing fresh film at all times, each bit of film is exposed to background only 3/8 second. The target will eventually cross all eight slots and record a spectrum for 1/8 degree, or 3/64 second, but the cost of this method is that target spectra are being recorded for only 1/8th the time, or recording time is lost by the same factor that background is reduced.

SECTION IV

INFRARED DETECTION

Lacking direct information on the infrared emission from the Project Meteor re-entry object, we can only establish the upper limit to the emission and the detectability from the melting point of the aluminum body, which is a five inch sphere, of about 130 cm^2 cross-sectional area. The melting point of aluminum is 933° K, and a black body of this area and temperature emits about 178 watts/steradian, but only 23 per cent of this lies below 3.0 microns in wavelength. If we assume a 24-inch diameter telescope of 100 per cent optical efficiency at a range of 100 miles (1.61×10^7 cm), the radiation collected amounts to 4.6×10^{-10} watts (below 3 microns).

A typical uncooled PbS cell of 1 mm^2 area, chopped at 100 cps, 4 cps bandwidth, has a noise equivalent power,

$$NEP \approx 3.0 \times 10^{-12} \text{ watts.}$$

Thus, this cell is capable of responding to this radiation even at 100 miles range. However, care must be exercised to restrict the angular field of the background emission in the infrared from the lower atmosphere (see Figure 5B, Section I,F). Making the crude assumption that this atmospheric background is representable by a black body at 260° K, the same 24-inch telescope below 3 microns will pick up 2.4×10^{-10} watts per square milliradian of field of view.

Although these crude estimates only indicate the order of magnitude of the problem, it again appears that rather accurate tracking of the IR telescope will be required to keep the background to a tolerable level. An alternate system would consist of a large mosaic of PbS cells, each viewing only a small field of view and operating a separate amplifier and recorder.

The signal intensity will fall off very rapidly at lower temperatures, since, in addition to the fourth power decrease, the wavelength distribution will shift the majority of the radiation beyond 3 microns out of the range of the PbS cell.

DOCUMENT CONTROL DATA – R&D

(Security classification of title, body of abstract and indexing annotation must be entered when the overall report is classified)

1. ORIGINATING ACTIVITY *(Corporate author)*
Geophysics Corporation of America under P.O. No. A-2231 to Lincoln Laboratory, M.I.T.

2a. REPORT SECURITY CLASSIFICATION
Unclassified

2b. GROUP
None

3. REPORT TITLE
Effect of Night Sky Backgrounds on Optical Measurements

4. DESCRIPTIVE NOTES *(Type of report and inclusive dates)*
Final Report

5. AUTHOR(S) *(Last name, first name, initial)*
Chapman, R.M. and Carpenter, R.O'B.

6. REPORT DATE	7a. TOTAL NO. OF PAGES	7b. NO. OF REFS
6 March 1959	66	14

8a. CONTRACT OR GRANT NO.
AF 19(604)-4559

b. PROJECT NO.

c.

d.

9a. ORIGINATOR'S REPORT NUMBER(S)
Final Report

9b. OTHER REPORT NO(S) *(Any other numbers that may be assigned this report)*
ESD-TDR-66-168

10. AVAILABILITY/LIMITATION NOTICES
Distribution of this document is unlimited.

11. SUPPLEMENTARY NOTES
None

12. SPONSORING MILITARY ACTIVITY
Air Force Systems Command, USAF

13. ABSTRACT

A review is given of the sources and magnitudes of the night sky backgrounds, from 0.3 to 5 microns particularly as they might interfere with the observation of the spectrum of a small missile re-entering the atmosphere. Distributions of stellar magnitude and color, zodiacal and galactic scattered light, air glow, twilight, moonlight, and man-made lighting are discussed.

Application is made of the background magnitude data to estimate the limitation of the threshold of large telescope-spectrometers using 1P21, PbS, and other detectors. Objective and slit-type spectrographs are considered, including the requirements for, and effect of, tracking precision.

14. KEY WORDS

re-entry vehicles
night sky background
optical measurements
telescopes
spectrometers
point sources
Cassegrain
photomultiplier
spectrograph
infrared detection